January 2019

The Application Of Extracorporeal Photochemotherapy To Head And Neck Squamous Cell Carcinoma

Alp Yurter

The Application of Extracorporeal Photochemotherapy to Head and Neck Squamous Cell Carcinoma

A Thesis Submitted to the

Yale University School of Medicine

in Partial Fulfillment of the Requirements for the

Degree of Doctor of Medicine

by

Alp Yurter

Graduating Class of 2019

TABLE OF CONTENTS

ABSTRACT

Extracorporeal Photochemotherapy (ECP) is an FDA-approved immunotherapy that has been treating cutaneous T cell lymphoma (CTCL) for over three decades. ECP's antitumoral effect is a consequence of its generation of functional, physiologic, inflammatory monocyte-derived dendritic cells (MoDCs) and apoptotic, patient-derived tumor, which collectively, stimulate the adaptive immune system. Thus, in CTCL, ECP serves as a therapeutic dendritic cell vaccine against patient-specific neoantigens. This mechanism of action suggests ECP's potential application to other solid tumors. We tested ECP's applicability to head and neck squamous cell carcinoma (HNSCC) using a trackable antigen system involving the constitutively expressed HPV16 E7 oncoprotein. We hypothesized that ECP would successfully stimulate anti-epitope CD8 T cells, quantified by IFN-gamma ELISA, following processing and cross-presentation of HPV16 E7+ peptides and tumor cells by MoDCs. The trackable antigen system employed a commonly cited epitope, $E7_{(11-19)}$. E7+ short peptide and long peptide generated significant IFNg ($p<0.0001$) relative to the null control group. Tumor cell line SCC61 T+ ($E7^{hi}$) demonstrated significantly elevated IFNg production relative to SCC61 T- (non-E7 expressing tumor), but only in the presence of platelets, plate-passage, and overnight incubation ($p<0.0001$). These results suggest an antigen-specific CD8 T cell response and reiterate critical ECP components that have previously been shown to facilitate immunogenic MoDC generation. Immunogenic MoDC phenotype was confirmed with flow cytometry of inflammatory surface markers and intracellular cytokines, all of which were generally upregulated following ECP. Overall, we have demonstrated a proof-of-principle for ECP's therapeutic vaccination against HNSCC. This is particularly relevant because ECP offers unique synergistic potential with recently FDA-approved checkpoint inhibitors.

ACKNOWLEDGEMENTS

Working in Dr. Richard Edelson's lab was my most memorable academic experience in medical school. I fortuitously found my mentor's lab in my search for a basic science cancer immunotherapy project following my first year of medical school. After completing my summer project, I knew I would return for a fifth-year research experience.

Dr. Richard Edelson and Dr. Douglas Hanlon were my primary mentors. Dr. Edelson oversaw the "big picture". Without him, this project would not be possible and I would not have the privilege of working with experts in this field. Dr. Douglas Hanlon and Dr. Olga Sobolev provided their expertise in immunology and subsequently guided the experimental designs. They also helped in interpreting the results. Eve Robinson, Renata Filler, and Dr. Kazuki Tatsuno provided their specialized knowledge to fine-tune experiments. Dr. Olga Sobolev, Eve Robinson, Dr. Douglas Hanlon, Renata Filler, Dr. Kazuki Tatsuno, and Patrick Han all assisted with running various aspects of the experiments.

The Yarbrough Lab (Dr. Wendell Yarbrough, Dr. Natalia Issaeva, and former members/classmates Cassie Pan and Tejas Sathe) generously collaborated with us on this project, providing materials and head and neck squamous cell carcinoma expertise.

The Hinrichs Lab at the NCI/NIH (Dr. Christian S. Hinrichs, Dr. Benjamin Jin, etc.) generously collaborated with us, providing materials for T cell transductions and expertise in T cell manipulation.

Inger Christiansen and the rest of the nurses of the photopheresis unit generously drew donor blood.

Antonella Bacchiocchi and Dr. Ruth Halaban generously provided a working space in which to transduce T cells.

Funding support for this thesis was provided by the James G. Hirsch, M.D., Endowed Medical Student Research Fellowship.

INTRODUCTION

An improved understanding of the relationship between immune system dysfunction and the development, establishment, and progression of cancer has evolved the landscape of immunotherapy.[1] In an immunocompetent host, if the immune system is able to recognize the cancer cell as "foreign" and avoid suppression, it should succeed in eradicating the malignancy. A high tumoral mutation rate increases the probability of generating non-synonymous mutations, and consequently, targetable neoantigens on the cell surface.[1-3] Interestingly, extracorporeal photochemotherapy or extracorporeal photopheresis (ECP), an FDA-approved immunotherapy for advanced cutaneous T cell lymphoma (CTCL), serves as a therapeutic dendritic cell vaccine which generates a clinically significant cytotoxic T-cell response against patient-specific neo-antigens.[4,5] This unique capability theoretically extends ECP's application to other malignancies[4-8], particularly those with high mutation rates or poorly characterized molecular targets.[2,3,9,10]

ECP Discovery

Edelson and colleagues serendipitously discovered the clinical effects of ECP when they were devising a blood-directed palliative chemotherapy against CTCL, a group of non-Hodgkins lymphoma marked by skin infiltrating malignant T cells.[11,12] The first patient treated with ECP in 1982 entered lifelong remission after only 3 monthly treatment cycles of 3% of the total CTCL cells.[5] Furthermore, in the 1987 phase I/II clinical study treating 37 resistant CTCL patients, although less than 5% of the patient's malignant T cells were treated with photochemotherapy, 73% of the patients responded to treatment and experienced an average 64% decrease in cutaneous involvement. Remarkably, there were no serious side effects.[11] As a result of this favorable trial, ECP was expeditiously approved by the FDA in 1988, and subsequently, CTCL was no longer deemed a universally fatal disease.[5,12]

ECP's Mechanism of Action

The cellular and cytokine interactions involved in ECP's immunogenic effect have slowly been defined

over the course of several decades since its invention. Edelson and colleagues surmised that the clinical effects of ECP could not be explained simply by the reduction in the population of circulating malignant cells, since less than 5% of the patients involved T cells were exposed to the photochemotherapy. ECP's mechanism of action became even more nebulous after the medical community realized its beneficial immunosuppressive effects in organ transplant recipients (ie graft versus host disease or transplant rejection)[13], suggesting bidirectionality of ECP's immunomodulation. It was not until the discovery that ECP was able to generate two maturationally distinct subsets of dendritic cells, one immunogenic and one immunotolerizing[4,5,14-16] that this seemingly paradoxical phenomenon was reconciled.

Understanding of ECP's immunogenic mechanism requires summarizing the therapy's use in CTCL:
(1) A portion of the patient's whole blood is removed and the leukocyte fraction containing malignant CD4 T cells, healthy immune cells and platelets is isolated and combined with 8-methoxypsoralen (8-MOP).
(2) This cellular/chemotherapy mixture is exposed to UVA radiation as it passes through a 1mm channel within parallel plastic plates permeable to UVA. UVA light activates 8-MOP into the therapeutically active form capable of cross-linking DNA and thus inducing cell death through DNA damage. The photochemotherapy combination, UVA and 8-MOP (PUVA), is titratable, so that it can preferentially induce apoptosis of leukocytes (ie malignant cells in CTCL) while sparing other immune cell subsets such as monocytes and dendritic cells.
(3) The cell mixture is returned to the patient, inducing an immunogenic response against the malignancy.

The current understanding of ECP's mechanism, deriving from years of scientific research, and endorsed by the ECP community at the recent meeting of the American Council of ECP[17], is as follows.

A. Platelet-Monocyte Interactions Produce Monocyte-Derived Dendritic Cells

As the cells and plasma proteins pass through the parallel plates during ECP, fibrinogen coats the surface of the polystyrene flow chamber, and platelets subsequently adhere to the RGD domains of fibrinogen via

αIIβ3 and α5β1 receptors. The adherent/activated platelets translocate P-selectin among other proteins to their surface, which then binds monocytes via PSGL-1, facilitating monocyte tethering to the platelets, partial monocyte activation, and monocyte integrin receptor conformational changes. Further interactions between platelet ligands (including those containing RGD domains) and monocytes induce monocytes into the dendritic cell (DC) maturational pathway. Flow shear stresses imparted on tethered monocytes, and platelet density within the ECP plate, are significant factors in transforming monocytes into monocyte-derived dendritic cells (MoDCs).[5,7,18]

B. PUVA Effect on Antigenicity and Dendritic Cell Maturation

Concurrent to monocyte activation by platelets, 8-MOP becomes transiently photoactivated upon UVA exposure, covalently crosslinking pyrimidine bases of DNA and irreversibly damaging exposed nucleated cells. In ECP, the 8-MOP-UVA (PUVA) dosage is such that as few as three DNA-photoadducts per million DNA base pairs can induce universal lymphocyte apoptosis, while largely sparing the similarly exposed monocytes.[5,19]

In CTCL patients, platelet-monocyte interactions produce functional, immunogenic MoDCs, which uptake PUVA-induced apoptotic malignant lymphocytes as a patient-specific antigen source, and produce a clinically significant CD8 T cell response against the malignancy.[5,7,8,11,12,20] Within 24 hours of ECP, monocytes increase expression of 498 genes, nearly 20 of which are associated with mature DC function and identity, and over 60 encoding for transmembrane signaling proteins. In particular, RNA transcripts coding for MHC class II presentation (ie DC-LAMP), T cell costimulatory molecules (ie CD80, CD86, CD40), and other DC maturation markers (ie CD83, Decysin, FPRL2, CCR7, Decysin, OLR1) have been shown to be significantly upregulated.[12] The immunogenic ECP-derived MoDCs upregulate surface expression of CD83, CD36, and MHC class II molecules, while reducing expression of CD14. Most importantly, these DCs acquire the functional capacity to mediate antigen cross-presentation to CD8 T cells and induce antigen-specific T cell proliferation.[5,7] In addition, tumor cells treated with PUVA

upregulate MHC class I molecule (MHCI) expression and therefore, along with uptake by ECP-derived MoDCs, also enhance neoantigen peptide processing, improving the TCR-mediated CD8 T cell response.[21]

In contrast, if monocytes themselves are sufficiently damaged by PUVA, they instead become immature, tolerogenic DCs.[16,22-24] Under these conditions, PUVA-exposed monocytes upregulate the glucocorticoid-induced leucine zipper GILZ (a hallmark of tolerogenic DCs), downregulate costimulatory molecules CD80 and CD86, exhibit resistance to Toll-like receptor-induced maturation, increase production of IL-10, and decrease production of IL-12.[22] Additionally, PUVA can result in DC apoptosis, which furthers the immunosuppressive environment by inducing regulatory T cells. These cellular mechanisms are thought to underlie ECP's immunotolerizing effects in GvHD and organ transplant patients.[16]

C. MoDCs Generate an Antigen-Specific Response

Current understanding of dendritic cell biology and ECP's favorable clinical results in the absence of major systemic side effects suggest patient-specific antigen targeting by T cells, with recent murine and in vitro studies confirming this.[4-6,8,20,25] Immunogenic ECP drives an adaptive immune response against patient-specific neoantigens, primarily through antigen-containing MoDC activation of CD8 T cells, though the presence of CD4 T cells and natural killer cells have also recently been shown to be significant factors in the anti-tumor effect.[4] In tolerizing ECP, tolerogenic MoDCs are thought to achieve antigen-specificity though uptake of non-self antigens arising from tissue damage in GvHD or transplant settings, and specific stimulation of regulatory T cells.[5,16,22]

ECP's Evolution

To improve MoDC maturation and neoantigen uptake, processing, and docking onto APC's MHC molecules, studied in the early 2000's onward adopted a modified ECP protocol termed "Transimmunization" (TI), which includes an overnight incubation period of PUVA-treated cells.[4,6,8] During this period, spatial proximity of PUVA-damaged tumor cells with platelet-activated MoDCs

allows for more efficient DC uptake and processing of antigens from dying tumor cells, as evidenced by a 60% clinical response rate of CTCL patients who failed standard ECP and/or other therapies during a clinical trial of Transimmunization for CTCL.[26] Furthermore, ECP's ability to provide a functional, therapeutic DC vaccine against undefined patient-specific neoantigens suggests therapeutic potential against other solid tumors. A modified transimmunization protocol where only tumor cells but not immune cells are exposed to PUVA, and where PUVA-treated tumor cells are subsequently co-incubated with MoDCs prior to re-injection, has recently demonstrated a significant CD8 T cell response against melanoma antigens both ex vivo and in vivo,[4,20] with melanoma (YUMM1.7)-inoculated and colon carcinoma (MC38)-inoculated mice exhibiting significantly reduced tumor volume relative to untreated controls.[4]

Potential Application to Head and Neck Squamous Cell Carcinoma

To test ECP's efficacy in other solid tumors, we sought a malignancy with poor prognosis and easily trackable antigens to demonstrate therapeutic vaccination proof-of-principle. Head and neck squamous cell carcinoma (HNSCC) accounts for 550,000 cases and 380,000 deaths annually. One-third of patients present with early stage disease (stage I or II). These patients, managed with primary surgery or radiotherapy (RT), carry a five-year overall survival rate of 70-90%. The remaining two-thirds of patients present with locoregionally advanced disease (stage III or IV) and are treated with a combination of surgery, RT, and/or chemotherapy. Unfortunately, 60% in this latter group experience local recurrence and 30% demonstrate distant metastases. Those with recurrent or metastatic disease have a median overall survival of 10 months.[1,27-29] HNSCC's robust immunosuppressive mechanisms explain the particularly poor prognosis, at least in part due to the following: generation of regulatory T cells, dysfunctional antigen processing and presentation, dysregulation of cytokine and chemokine pathways, and a hostile tumor microenvironment.[1,27,30,31]

HNSCC can be further classified into human papilloma virus (HPV) positive and negative entities, with 25% of all HNSCC and up to 90% of oropharyngeal carcinoma cases being HPV positive.[29,30,32] It is well established that carcinogenic strains of HPV are responsible for the constitutive synthesis of oncoproteins E6 and E7, inhibitors of tumor-suppressor proteins p53 and Retinoblastoma (Rb), respectively.[33] Because these oncoproteins are uniquely expressed on malignant tissues, they have become attractive therapeutic targets,[30,33-35] and at minimum, can serve as trackable tumor-specific antigens for demonstrating ECP's applicability to HNSCC.

We hypothesized that ECP could be a potent therapy against HNSCC given the recent success of adoptive tumor-infiltrating lymphocyte (TIL) transfer strategies in this disease.[3,10,30,36] In fact, Stevanovic et al. found in patients an immunodominant T cell reactivity against neoantigens, rather than the canonical E6 and E7 epitopes,[3] which favorably plays into ECP's unique mechanism of action.[5] Moreover, PUVA's ability to upregulate MHCI expression[21] may partially overcome the immunosuppressive nature of HNSCC.[1] Finally, the recent FDA-approval of checkpoint inhibitors directed against PD-1 and CTLA-4 receptors on T cells further increased the ECP's appeal, offering potential for immunotherapeutic synergism between a dendritic cell-based strategy and immunogenic T cell activation strategies.[1]

Here, we investigated ECP's potential to treat HNSCC through the *in* vitro generation of a CD8 T cell response against a well-established HPV16 E7 epitope using the TI protocol. In selecting a trackable antigen, we focused on HPV16 because it is the most commonly implicated HPV strain in HNSCC.[29,30,32] With respect to oncoprotein, we chose E7 instead of E6, given that it exhibits less sequence variation and has superior epitope binding affinity to HLA*A2:01, the most prevalent MHCI molecule in the United States and Europe.[30,37,38] With respect to CD8 T cell receptors, we sought epitope specificity to $E7_{(11\text{-}20)}$ and $E7_{(11\text{-}19)}$, highly studied sequences with ability to stimulate CD8 T cells in vitro and in vivo.[38,39] We reasoned that if ECP is able to initially demonstrate successful proof-of-principle CD8 T cell response specifically against HPV antigens in HNSCC, then the therapy may similarly generate an *in vivo* response

against patient-specific HNSCC neoantigens, which are implicated in clinically effective anti-tumor responses.[3,5,9] This is the first time ECP has been tested in the context of HNSCC.

STATEMENT OF PURPOSE

This is a proof-of-principle project to determine ECP applicability to HNSCC by using a trackable antigen source, in particular, two commonly studied immunogenic HPV16 E7 epitopes.

Specific Aims

1. Generate a CD8 T cell line with TCR specificity to HPV16 $E7_{(11-19)}$ and $E7_{(11-20)}$ epitopes

2. Demonstrate that the updated "Transimmune" version of ECP (TI) can generate an HPV16 E7 Ag specific CD8 T cell response using HPV16 E7 overlapping and long peptides

3. Demonstrate that TI can generate an HPV16 E7 Ag specific CD8 T cell response using a HNSCC cell line expressing E7 protein

4. Demonstrate that following TI, monocytes acquire a mature, immunogenic DC phenotype, which underlies successful Ag cross-presentation

Hypothesis

TI will generate functional, immunogenic MoDCs, defined by their ability to phagocytose, process, and cross-present HPV+ HNSCC antigens, thus stimulating CD8 T cells in an antigen-specific manner.

MATERIALS AND METHODS

HPV16 E7 Antigen Sources

Peptides. Short, long, and overlapping peptides of the HPV16 E7 protein were used as Ag sources. Short peptide (SP) can directly fit into the TCR groove, bypassing APC phagocytosis, processing, and loading onto MHCI. Because of this capacity to directly stimulate T cells, SP served as a positive control. In contrast, long and overlapping peptides served as the experimental Ags, as they require functioning APCs for CD8 T cell stimulation.[39] Short peptides: 9mers (amino acid sequence: YMLDLQPET) and 10mers (amino acid sequence: YMLDLQPETT) were synthesized at Tufts School of Medicine. Long peptide (LP): HPV16 $E7_{(1-30)}$ was synthesized at Tufts School of Medicine. Overlapping peptide (OP): PepMix™ HPV 16 Protein E7, a commercially available pool of 22 peptides derived from a peptide scan (15mers with 11 aa overlap) was used (JPT Peptide Technologies). Nanoparticle encapsulation: Using a previously described protocol**,** LP and OP was encapsulated with PLGA, which has been shown to enhance APC phagocytosis and presentation of the MHCI-peptide complex.[40] SIINFEKL (ie $OVA_{257-264}$) and melanoma antigen $gp100_{(25-33)}$ were used as negative peptide controls.

Cell Lines

Two SCC61 cells, one transfected to express high levels of HPV16 E6/E7 proteins (SCC61 T+) and one non-transfected and naturally non-expressive (SCC61 T-), were grown in DMEM/F12 media (1:1) + 10% FBS + 0.4ug/ml hydrocortisone.[41] The SCC090 cell line (SCC90), naturally expressing HPV16 E7 protein, was purchased at ATCC and grown in MEM, 10%FBS, 2mM L-glutamine. Normal human fibroblasts (NHF), which served as a cell line based negative control for E7 Ag, and NHF line modified to express HPV16 E6/E7 proteins (NHF T+) which served as a non-tumoral cell line source of E7 Ag, were grown in DMEM, 10%FBS, 2mM L-glutamine. SCC61 T-, SCC61 T+, NHF, NHF T+ were generously donated by the Yarbrough Lab at Yale. All cell lines were grown with Pen/Strep and grown to 70-80% confluence, harvested with trypsinization, and centrifuged at 1400RPM for 7min prior to use.

Peripheral Blood Mononuclear Cells (PBMCs)

PBMCs were obtained from healthy, HLA*A2:01+ human donors, in accordance with the guidelines of the Yale Human Investigational Review Board, and with informed consent obtained under protocol number 0301023636**.** Whole blood was collected at a ratio of 100ml whole blood to 500ul heparin, so as to prevent coagulation but preserve future platelet activation. Whole blood was gently layered over Isolymph (CTL Scientific Supply Corp.) at a ratio of 35ml:15ml, centrifuged for 30minutes at 1500rpm. Then, the buffy coat was collected, washed with PBS using the same centrifugation settings, and the PBMC pellet resuspended for use.

CD8 T Cells

Anti-HPV16 E7$_{(11-20)}$ CD8 T cells. CD8 T cells with anti-HPV16 E7$_{(11-20)}$ TCR specificity were obtained from a commercial line originating from a female HLA*A2:01+ donor (Astarte Biologics), and expanded using the rapid expansion protocol (below). Following expansion, CD8 T cell purity was determined with flow cytometry analysis (below).

Anti-HPV16 E7$_{(11-19)}$ CD8 T cells. Transgenic CD8 T cells with anti-HPV16 E7$_{(11-19)}$ TCR specificity were generated from a healthy, middle-aged, male HLA-A2+ donor's PBMC population (**Supplementary Figure 1**). CD8 T cells were isolated from PBMCs, transduced to co-express anti-E7$_{(11-19)}$ TCR, and expanded using a rapid expansion protocol (REP). Following expansion, CD8 T cell purity was determined with flow cytometry analysis.

TCR retroviral constructs. A retroviral supernatant capable of transducing human T cells to co-express TCRs with high-affinity binding to the E7$_{(11-19)}$ epitope was generously donated by Dr. Christian Hinrichs and his colleagues (NCI). The supernatant contains MSGV1 retrovirus, modified to include TCR nucleotide sequences inserted into its retrovirus backbone and is codon-optimized for expression in human cells. Moreover, its human TCR constant regions are exchanged for mouse TCR constant regions,

allowing for easy flow cytometry confirmation of successful transduction. This retrovirus has been used in prior clinical trials (Gene Oracle) and its molecular structure has been extensively characterized.[30]

T cell transduction. Retroviral transduction was carried out based on recommendations from the Hinrichs Lab. On day 1, human PBMCs were isolated from a healthy HLA-A2+ donor and CD8 T cells were isolated using negative selection (Miltenyi Biotec). CD8 T cells were seeded into three wells of a tissue-culture 24-well plate at a ratio of $7.5x10^6$ CD8 T cells per well, with each well containing 2ml media (50/50 media + 300 IU/mL IL2 + 50 ng/mL OKT3). On day 2, a non-tissue culture 24-well plate was coated with retronectin (Takara #T100A/B) at final concentration of 20 µg/ml in PBS (ie 500ul retronectin/well), wrapped and stored overnight at 4°C. On day 3, the retronectin plate was centrifuged at 2000xg at 32°C for 1 hour, followed by retronectin solution aspiration and blockage with 2ml 2% BSA in PBS for 30min at room temperature (RT). The retroviral supernatant was spun for 10 minutes at 1000RPM. The retronectin plate was washed 2x with 1ml/well PBS, with the PBS remaining until the viral supernatant was added. After the 0.5ml/well supernatant was added, the retronectin plate was plastic wrapped, and spun for 2000xg at 32°C for 2 hours. At the 1.5hour mark, T cells from the other plate were harvested and counted. The retronectin plate's supernatant was aspirated and $0.25x10^6$ T cells were added/well in 1 ml of media (50/50 AIMV/RPMI + 300 IU/mL IL2). The plate was wrapped and spun for 10min at 1500RPM with brake set at 1, and incubated overnight. On day 4, the transduced cells were transferred off the retronectin into a tissue culture-coated 24-well plated. On day 6, cells were transferred to the appropriate sized flask and replenished with T cell media. On day 7, flow cytometry was used to assess $E7_{(11-19)}$ TCR positivity (below).

Cell Sorting. T cells were harvested, spun down for 10min at 1500RPM, supernatants were discarded, and the cells were resuspended. Fc block was added and cells were incubated for 15min on ice. Staining buffer (1xPBS w/3% BSA) was added, and cells were centrifuged and resuspended identically. Samples

were stained for anti-CD8-BV421, anti-CD3-APC, anti-mTCRb-FITC (clone: H57-597), anti-7AAD-percp-cy5.5, with respective single stain controls; stained cells were incubated for 30min on ice. Cells were centrifuged and resuspended identically, passed through a 70um filter (Falcon), and brought up at a $25x10^6$/ml sorting buffer (1xPBS w/ 0.1% BSA). Live CD3/CD8/mTCR-β triple-positive were selected (BD FACSAria).

Rapid Expansion Protocol (REP) of CD8 T cells. REP stimulates T cells with the monoclonal antibody OKT3 (anti-CD3), IL-2, and irradiated autologous or allogeneic feeder cells to expand lymphocytes up to 1000-fold over 14 days. This protocol was used to expand both $E7_{(11-19)}$ and $E7_{(11-20)}$ CD8 T cells. Approximately $2x10^8$ feeder cells (ie PBMCs) were obtained from 3 healthy HLA-A2+ donors using the methods above and subsequently irradiated with 4000cGy (Yale Cesium-137 irradiator) at a cell concentration of $50*10^6$/ml on ice. $2x10^8$ feeder cells were combined with $1\text{-}2x10^6$ CD8 Tcells in a T-150 with the following "50/50" media components: 75ml "complete media" (10% human AB serum (Lonza), pen/strep, 2.5% HEPES in RPMI), 75ml AIM V media, 4.5ul OKT3 (1mg/ml), 75ul IL-2 (1300IU/ml), ciprofloxacin (10 ug/ml). This flask was incubated at 37°C, 5% CO2 until day 5, during which 3/4 of the medium was aspirated without disturbing the settled cells, and replenished with fresh 50/50 medium (as above) but *without* OKT-3. From this point forward, when the viable cell count reached $0.6x10^6$-$1x10^6$/ml, the cells were split 1:2 and replenished with AIMV media with 5% human AB serum and 1300IU/ml IL-2. Cell count was assessed every two days. The desired effector T cell population was confirmed with flow cytometry (below) and frozen down at $5x10^6$/ml 10% DMSO aliquots in liquid nitrogen.

Flow cytometry to characterize post-REP CD8 T cells. Flow cytometry was used to confirm the epitope-specific T cell population following REP. Fixable apoptosis dye "zombie"-apc-cy7, anti-mTCRb-FITC, anti-$E7_{(11-20)}$ dextramer-PE, anti-CD8-PacBlue, anti-CD4-PE-Cy5.5, and anti-CD3-APC stains with respective IgG controls were used (Biolegend). Anti-HPV $E7_{(11-19)}$ CD8 T cells were identified based on

the live CD3/CD8/mTCRβ positive population. Anti-HPV $E7_{(11-20)}$ CD8 T cells were identified based on the live CD3/CD8/$E7_{(11-20)}$ dextramer positive population. Data were acquired with a Stratedigm flow cytometer (BD Biosciences) and analyzed with FlowJo software (FlowJo).

Transimmunization (TI) procedure

The TI employed closely followed a previously established protocol,[4] but was adjusted for different cell lines. An overall schematic is available as **Supplementary Figure 2.** Briefly, PBMCs were combined with PUVA-treated tumor cells, plate-passaged together, and incubated overnight. For peptide Ag groups, PBMCs alone were passed over a plate and peptide was added directly to the overnight incubation dish. The effects of plate passage, platelets, and TI (ie plate passage and overnight incubation) on T cell stimulation were tested. Additionally, each PBMC + CD8 Tcell + Ag group had parallel Ag groups containing only CD8 T cells or only PBMCs. Allogenic PBMCs were used in $E7_{(11-20)}$ experiments while autologous PBMCs were used in $E7_{(11-19)}$ experiments.

CD8 T cell Thaw (Day 0). CD8 T cells were thawed and spun down at 700 RPM for 7 minutes. They were counted and incubated in T-25 flasks with 20ml T cell media (5% human AB serum, pen/strep, 2mM L-glutamine in AIMV) and 8ul/20ml media of 1300IU/ml IL-2 until Day 2.

PUVA (Day 1). The PUVA dose was cell line specific and based on the minimum dosage required to induce 100% apoptosis. Apoptosis was assessed by proliferation cessation during a 10-day monitoring period under confocal microscopy. SCC61 T+, NHF T-, and NHF T+ were treated with 8 Joules(J)/cm^2 and 200ng/ml 8-MOP while SCC61 T-, SCC90 were treated with 4J/cm^2 and 200ng/ml 8-MOP. NHF T+ served as non-tumoral cell source of E7 Ag while NHF T- served as a non-antigenic negative control cell line. Cell lines were trypsinized, centrifuged and brought up at a concentration of $2.5x10^6$ cells/300ul FBS. They were incubated in the dark with respective amounts of 8-MOP for 20minutes. To prepare for UVA treatment, 12-well plates were pre-coated with FBS to prevent cell adhesion. When 8-MOP

incubation was completed, FBS was aspirated from the wells, and each well received $2.5x10^6$ cells. Finally, each cell line received their respective UVA dose.

Plate passage (Day 1). For groups involving cell lines as an Ag source, PUVA treated cells were combined with 10^7 cells PBMCs for a total volume of 600ul FBS. For groups involving peptides as an Ag source or PBMC + Ag groups, up to $4x10^7$ cells PBMCs were brought up in 600ul FBS. For all groups, two-thirds (400ul) of the 600ul were used to coat the micro-plates for an hour at 37°C to maximize fibrin and platelet adhesion; the remaining one-third remained in the Eppendorf tube. Microplate tubing was coated with FBS to prevent cell loss. After one hour, 600ul of cells were passaged through the microplate at 0.09 ml/min using a syringe pump. After collecting cells into respective Eppendorf tubes, microplates were washed with FBS at 0.49 ml/min in order to maximize cell yield. Overall, plate passage closely followed a previously established protocol.[4]

Overnight Incubation (Day 1). To maximize MoDC maturation and Ag uptake, cell groups were incubated overnight at 37°C. After plate passage, cells were counted. The cell count across groups were normalized based on the group with the lowest yield, typically above $5x10^6$ cells, and each cell group was transferred into a respective 35mm dish with 15% human AB serum in 2ml RPMI. Groups that were not plate-passaged were thrown into the 35mm at the same time as their plate-passaged counterparts. In general, peptides were added at 10uM concentration into their respective dishes; however, nanoparticle encapsulated particles were added at a concentration of 200ug NP/2ml RPMI, based on prior NP experiments.[40]

CD8 T Cell Co-Culture (Day 2). The next day, PBMCs in 35mm dishes and effector CD8 T cells were harvested, spun down, brought up in TCM, and counted. All groups were seeded as triplicates in 96-well plates for a total volume of 200ul TCM/well. For PBMC + T cell + Ag groups, 100ul of $0.2x10^6$ PBMCs

were combined with 100ul of $0.1x10^6$ effector CD8 T cells. PBMC + Ag and T cell + Ag groups seeded $0.2x10^6$ PBMCs in 200ul TCM and $0.1x10^6$ CD8 T cells in 200ul TCM/well, respectively. In the T cell + Ag groups, peptide Ags were added at 10uM as before, and cell lines were PUVA treated and added in proportional numbers to their respective day 1 groups. Coincubation in the 96-well plates lasted 72 hours.

Platelet depletion and "No TI". In experiments involving transgenic CD8 T cells, the immunogenic contributions of platelets and TI were investigated. On day 1, platelets were depleted using CD61 microbeads (Miltenyi Biotec) following PBMC isolation. Platelet depletion was confirmed using a Hemavet (Drew Scientific, Inc.), with a threshold of $<10^4$/ul considered successful depletion. Moreover, autologous serum (BD Vacutainer) was used for overnight incubation media. Subsequent experimental distribution of platelet-containing and platelet-depleted PBMCs was the same as above. The "no TI" effect was explored by acquiring fresh PBMCs on day 2 and platelet-depleting a portion of them as done with TI, and adding them to a PBMC + T cell + Ag co-culture without plate passage and overnight incubation. "No TI" PBMCs were distributed to their respective groups as described in the "*CD8 T Cell Co-Culture"* section above.

Monocyte Isolation. To simplify the APC-T Cell co-culture system and background IFNg noise, monocytes were isolated from donor PBMCs using the Pan Monocyte Isolation Kit (Miltenyi Biotec) per manufacturer's recommendations. In the $E7_{(11-20)}$ system, monocytes were purified either on the day of PBMC isolation or after overnight incubation and prior to 96-well plate transfer. In the $E7_{(11-19)}$ system, monocytes were purified immediately following PBMC isolation.

Cell Stimulation Readouts

IFNg ELISA to measure CD8 T cell stimulation. After 72 hour co-cultures, the 96-well plates were spun down at 2000RPM for 10min at 4°C. 180ul of supernatant were transferred into new 96-well plates,

wrapped, and frozen at -80C. Supernatants were analyzed with ELISA for interferon-γ (IFNg) production (BioLegend), which signifies CD8 T cell stimulation.[30,42] The ELISA was run according to vendor guidelines and analyzed with the Spectromax reader.

Flow cytometry to characterize phenotypic changes in monocytes after TI. The following surface markers which characterize MoDC maturation[4,12,43] used to stain PBMC following TI treatment, per manufacturer's instructions: CD80-FITC, CD83-APC, CD86-PE, HLA ABC-APC, HLA-DR-APCEeFlour 780, CD11c-PE/Cy7, CD14-PacBlue, ICAM1-FITC, PLAUR-PE (BioLegend). An intracellular staining kit (BD Biosciences) was used to characterize associated chemokine expression with the following stains: CXCL5-PE, MCP-1-APC (BD Biosciences). Singlet, live, CD11c/CD14+ were gated on. Relative surface marker expression was quantified by change in mean fluorescent intensity (MFI) or by percentage of positive cells, as most appropriate to the stain. MFI was calculated as the intensity difference between stain and IgG. Percentage of positive monocytes was used to track populations expressing intracellular chemokines or surface CD80.

Flow cytometry to characterize PD-1 expression following T cell stimulation. PD-1 is a recently discovered surrogate for neoantigen-specific CD4 and CD8 T cell stimulation[3,36,44-46] and is therefore useful to ECP experiments, which involve mounting an adaptive immune response to undefined neoantigens. PD-1-PacBlue staining was used in conjunction with zombie-APC-Cy7, CD3-PE, CD4-APC, CD8-FITC, with corresponding IgGs (BioLegend) following 2 day stimulation with OKT-3 (30ul of 1mg/ml stock per 2ml media) and IL-2 (1300IU/ml) of PBMCs.

Statistics

Statistical analyses were performed with Prism 8 (GraphPad Software). Depending on the experiment, 1-way or 2-way ANOVA with Holm-Sidak's multiple comparisons test were used to determine statistically significant IFNg production with respect to antigen, nanoparticle, and/or plate-passage effects. Tukey's

multiple comparison tests were used to determine statistically significant differences in TI permutations in the $E7_{(11\text{-}19)}$ system. A *P* value of less than 0.05 was considered significant.

RESULTS

REP generates a large population of CD8 T cells with Desired TCR specificity.

To assess TI's APC cross-presentation efficiency, we first needed to generate two large populations of epitope-specific CD8 T cells using REP. Anti-HPV16 $E7_{(11-20)}$ CD8 T cells were expanded 200-fold from a commercially available 2 million cell aliquot, of which approximately 81% were viable epitope-specific CD8 T cells. Following REP, cells were 95% viable, with $E7_{(11-20)}$ CD8 T cells comprising two-thirds of the compartment (**Figure 1A**). Since the physiological relevance of the $E7_{(11-20)}$ epitope is not universally accepted by the HPV research community[38], we also generated in-house anti-HPV16 $E7_{(11-19)}$ CD8 T cells, and in this iteration, we sought a higher cell purity. After cell sorting, we obtained 1 million cells, nearly 100% of which were $E7_{(11-19)}$ CD8 T cell. After REP, cells were expanded 150-fold; up to 93% were viable, with $E7_{(11-19)}$ CD8 T cell comprising 95% of the compartment (**Figure 1B**).

CD8 T cells release IFNg upon direct stimulation with SP.

Following generation of epitope-specific CD8 T cell populations, we confirmed T cell functionality in the simplest IFNg assay, cognate SP stimulation. Both $E7_{(11-19)}$ and $E7_{(11-20)}$ T cell lines demonstrated appropriate IFNg release upon direct TCR stimulation with the appropriate SP. $E7_{(11-20)}$ T Cell cultures with antigen showed significant IFNg production exclusively with SP (**Figure 2A**: $p=0.012$; **Figure 2B**: $p<0.0001$). In contrast, non-specific gp100 or SIINFEKL peptides, or E7+ Ag sources requiring APC processing were not able to directly stimulate $E7_{(11-20)}$ T cells ($p>0.99$; **Figure 2**). $E7_{(11-19)}$ transgenic CD8 T cells also demonstrated significant IFNg release against their cognate SP (**Figure 2C**: $p<0.0001$).

Co-culture of PBMC with $E7_{(11-20)}$ CD8 T cells and E7 Ags results in non-specific IFNg production.

After demonstrating that our CD8 T cell lines could be stimulated with SP, we began TI testing of the $E7_{(11-20)}$ system to demonstrate APC-mediated Ag cross-presentation. PBMC + Ag cultures were run in parallel to the co-cultures to determine non-specific IFNg production (**Figure 3**), set as the dotted lines in

Figure 4. $E7_{(11-20)}$ CD8 T cells co-cultured with PBMC and peptide Ags (**Figure 4A**), did not significantly increase their IFNg production relative to the "null" (ie no Ag addition) group ($p>0.98$). When testing cellular E7 sources with the $E7_{(11-20)}$ T cell line (**Figure 4B**), again, there was no significant increase in IFNg production relative to the "null" group ($p>0.98$). Nanoparticle encapsulation and plate-passage did not significantly increase IFNg production ($p>0.98$ for both). Given that one-third of the "$E7_{(11-20)}$ CD8 T cells" added to the co-cultures were not epitope-specific (**Figure 1**), and the non-autologous co-culture system, we suspected that high IFNg levels even in the "null" control group were due to cross-reactivity between the impure compartment of $E7_{(11-20)}$ CD8 T cells and donor PBMCs. To minimize non-specific IFNg release, the peptide Ag experiment was repeated by isolating monocytes, the APC progenitor, from PBMC donors. The PBMC + $E7_{(11-20)}$ T cell + Ag experiment was run in parallel with the monocyte + $E7_{(11-20)}$ T cell + Ag experiment; corresponding monocyte groups had up to ~40x reduction in IFNg release, confirming our hypothesis of non-specific allogenic cross-reactivity in this system (data not shown). Initially, we planned to purify and REP $E7_{(11-20)}$ CD8 T cells for repeat experiments, but after speaking with HPV experts at the NCI (ie Dr. Christian Hinrichs and colleagues), we decided to instead move forward with the co-culture system involving $E7_{(11-19)}$ CD8 T cells, as $E7_{(11-19)}$, and not $E7_{(11-20)}$, is a naturally expressed epitope in HPV16 carcinoma. Additionally, this system used autologous PBMC as the source of APCs to minimize nonspecific reactivity.[38]

Co-culture of PBMC with $E7_{(11-19)}$ CD8 T cells and E7 Ags results in Ag-specific IFNg production. Overall, all E7+ groups seemed to selectively produce IFNg in the $E7_{(11-19)}$ system, suggesting successful TCR stimulation by direct exogenous loading as well as through APC-internalization/cross-presentation. First, a preliminary peptide stimulation assay was run comparing "null" no peptide, SP, and LP antigens in PBMC + $E7_{(11-19)}$ T cell + Ag co-cultures (**Figure 5A**). In this assay, autologous PBMCs were isolated and incubated overnight with 25uM of the relevant Ag, and the next day were transferred to a 96-well plate for 72 hour co-culture with T cells. Both SP and LP groups demonstrated over 40x IFNg production relative to the null group ($p<0.0001$). Further, the LP group produced significantly more IFNg than the SP

group ($p<0.05$). Next, a preliminary tumor stimulation assay was run comparing SCC61 T+ (**Figure 5B**) and SCC61 T- tumor cells as Ag sources (**Figure 5C**), and investigating the role of platelets in antigen-specific T cell stimulation**.** Following PBMC isolation, a portion of PBMC was platelet-depleted, and additionally, purified monocytes with and without platelets were prepared from PBMCs. $5x10^6$ PBMCs with or without platelets were pulsed overnight with $2.5x10^6$ PUVA-treated tumor cells prior to co-culture with $E7_{(11-19)}$ T cells. Significant IFNg release ($p<0.0001$) exclusively required the presence of platelets *and* an E7+ antigen source (**Figure 5B**). This preliminary experiment suggested that Ag from tumor cells could be efficiently cross-presented to anti-tumor T cells.

Following the initial confirmation of successful $E7_{(11-19)}$ T cell line stimulation with peptide and cellular antigens, a larger experiment investigating the role of TI (ie plate passage and overnight incubation) and platelets (PLT) in peptide and tumor Ag presentation was conducted (**Figure 6**). First, corresponding TI permutations of Ag groups were compared to that of the null group; the statistically significant differences are mentioned below. Negative control groups (null and SIINFEKL) exhibited similarly ($p>0.78$) minimal IFNg release across all tested TI groups. In contrast, positive control SP produced over 10x the maximum IFNg observed in the null group (red vertical asterisks; $p<0.0001$). With respect to LP, PLT-/TI- and PLT+/TI- groups demonstrated significantly elevated IFNg (red vertical asterisks; $p<0.0001$). Finally, the high E7-expressing SCC61 T+ tumor cell group demonstrated significantly elevated IFNg production in the PLT+/TI- ($p=0.043$) and PLT+/TI+ ($p<0.0001$) setups. Thus, groups containing E7+ peptide and tumor cells demonstrated antigen-specific CD8 T cell stimulation, as shown in the preliminary experiment.

To account for potential tumor-influenced inflammatory cytokine production[47], IFNg profiles of the E7 expressing groups were compared to those of the negative control cell line, SCC61 T-. The SCC90 group produced significantly less IFNg ($p=0.039$) in the PLT-/TI+ permutation but otherwise produced comparable levels to SCC61 T- ($p>0.09$). Notably, "full TI" SCC61 T+ (ie PLT+/TI+) produced significantly higher IFNg than its corresponding SCC61 T- group (red vertical asterisks; $p<0.0001$).

However, whereas the IFNg of the PLT+/TI- SCC61T+ was significantly higher than the null group (mentioned above), IFNg was similar to that of SCC61 T- ($p=0.103$). In this more conservative statistical analysis, the E7 expressing SCC61 T+ demonstrated antigen-specific CD8 T cell stimulation, but only with the "full TI" effect, underscoring the importance of platelets, plate-passage, and overnight incubation in producing inflammatory APCs capable of cross-presentation. Also of note, although the E7 protein is one of tens of thousands of proteins expressed within the SCC61 T+ cell line, its cross-presentation efficiency was remarkably efficient (nearly 50% as potent as pure peptide Ag preparations), confirming tumor-derived proteins as a viable source of personalized Ags for potential TI-based DC vaccinations in HNSCC.

We hypothesized that the increasing absence of critical "full TI" components (ie platelets (PLTs) or "TI" = plate-passage & overnight incubation) should progressively decrease Ag cross-presentation and thus CD8 T cell stimulation.[4,18] Tukey's multiple comparison tests revealed significant differences in IFNg release between TI permutations in the SCC61 T+ group (**Figure 6**: blue asterisks). Following the expected trend, PLT+/TI+ resulted in superior cross presentation relative to PLT+/TI- ($p=0.001$), PLT-/TI+ ($p<0.0001$), and PLT-/TI- ($p<0.0001$). SP (blue asterisk; $p<0.017$) and LP (blue asterisks; $p<0.003$) groups also exhibited significant variability across TI permutations, but not in the expected trend. Instead, there was higher T cell stimulation in the absence of TI, independent of the presence or absence of platelets. Given that both direct stimulation and cross-presentation requiring E7 peptide Ags demonstrated this phenomenon, CD8 T cell peptide stimulation results were likely confounded by proteolytic degradation (see discussion).

TI, platelets, and E7 Antigen sources induce a pro-inflammatory MoDC phenotype.

Monocytes in the $E7_{(11-19)}$ system were phenotyped for expression of the following inflammatory DC markers using a previously described panel[4] including: CD80, CD83, CD86, HLA-ABC, HLA-DR, ICAM1, PLAUR, CXCL5, and MCP-1 (**Figure 7**). Platelet-depleted and platelet-containing monocytes that had undergone TI (ie plate-passage and overnight incubation) with LP or with SCC61 T+ were

compared to monocytes from fresh PBMCs. The TI effect alone, regardless of Ag source or platelets, ostensibly resulted in an increased expression of every inflammatory marker tested except for HLA-ABC; monocytes undergoing TI with SCC61 T+ showed less relative surface expression of HLA-ABC. This seemed to be a phenomenon specific to tumor cell Ag, as monocytes in parallel LP and null groups instead exhibited increased surface density of MHCI (**Figure 7B**). Furthermore, the presence of platelets enhanced the degree of inflammatory marker expression across all parallel Ag groups except for MCP-1. Platelet-depleted null and SCC61 T+ groups exhibited higher MCP-1 expression than respective platelet-containing groups (**Figure 7I**). The groups with SCC61 T+ cells as antigen source showed the smallest upregulation of CD80, CD83, CD86, HLA-ABC, HLA-DR, and ICAM1 relative to null or LP groups (**Figures A-D, F-G**). On the other hand, SCC61 T+ monocytes exhibited the highest PLAUR surface expression (**Figure 7E**), and a distinctly larger subset of SCC61 T+ cell-pulsed monocytes were positive for intracellular chemokines CXCL5 and MCP-1 (**Figures 7H-I**).

PD-1 can be used as surrogate for T cell stimulation.

As previously mentioned, immunodominant antitumor T cell responses in HPV+ cancers are directed against neoantigens, and these TILs have been shown to reliably express PD-1. Given ECP's production of a neoantigen-based T cell response, we established a PD-1 staining system to detect populations of stimulated CD4 and CD8 T cells in future experiments involving undefined patient neoantigens. Following 2-day stimulation of healthy donor PBMCs with IL-2 and OKT-3, a potent CD3 receptor stimulator, 50% of the CD8 T cells were PD-1+, whereas unstimulated controls were only 7% PD-1+. CD4 T cells similarly exhibited an increase in PD-1+ from 12% to 57% after 2-day stimulation (**Figure 8**). At the time of this submission, post-stimulation PD-1 expression in HNSCC donor PBMCs has not yet been successfully determined.

DISCUSSION

We embarked on a proof-of-principle project to determine the potential of modified ECP procedure termed "transimmunization" (TI) to treat HNSCC, an entirely novel application of this immunotherapy. A miniaturized ECP system[4] was adopted to test whether CD8 T cells could be stimulated in vitro following APC cross-presentation of trackable HNSCC antigens, specifically, two commonly cited HPV16 E7 protein epitopes.[38,39,48] This work builds upon recent literature demonstrating ECP's capacity to generate a significant CD8 T cells in response to melanoma antigens in vitro[20] and in a murine model.[4] Given the crucial role of CD8 T cells in HNSCC regression and ECP's intrinsic ability to activate a cytotoxic T cell response towards patient-specific neoantigens, successful proof-of-principle would point to ECP's utility in providing a functional, therapeutic dendritic cell vaccine against undefined HNSCC antigens.

We first tested ECP's ability to stimulate $E7_{(11-20)}$ CD8 T cells since these readout cells were readily available commercially. Unfortunately, this system produced a large degree of non-specific IFNg and therefore could not be studied. We believe allogeneic immunoreactivity[49] (ie PBMC donor vs 67% pure commercial donor CD8 T cell with non-uniform TCR specificity) was a large contributor to the generation of IFNg observed in the PBMC + $E7_{(11-20)}$ T cell + Ag cultures; following monocyte isolation, monocyte + $E7_{(11-20)}$ T cell + Ag cultures generated an order of magnitude less of IFNg. To minimize future confounders, we planned to sort for a positive population $E7_{(11-20)}$ T cells and repeat experiments with monocyte depletion, as previously described.[20] However, separately, there was a major concern of poor natural cross-presentation of the HPV16 $E7_{(11-20)}$ epitope in human cells.[30] In fact, Riemer et al. demonstrated with MS3 Poisson detection mass spectrometry that the HPV16 $E7_{(11-19)}$ epitope, and not the HPV16 $E7_{(11-20)}$ epitope, was the highly-conserved peptide naturally complexed with HLA-A*0201, and able to direct T cell-mediated tumor cytolysis.[38] The immunologic relevance of the HPV16 $E7_{(11-20)}$ epitope was initially inferred from in silico predictions, HLA-synthetic peptide binding studies, and peripheral T cell functional activation assays, and not true identification of $E7_{(11-20)}$-MHCI complexes. In retrospect, the numerous failed clinical therapeutic vaccine trials of the early 2000's employing HPV16

$E7_{(11-20)}$ antigen support this notion.[35,38,39]

In the second phase of the project, we switched to an entirely autologous system involving the HPV16 $E7_{(11-19)}$ epitope to avoid the confounding factors mentioned above. First, a high purity transgenic CD8 T cell line co-expressing a high avidity anti- HPV16 $E7_{(11-19)}$ TCR was generated.[30] Functionality was confirmed by generation of IFNg with direct SP stimulation (**Figure 2C**). Interestingly, LP also stimulated T cells in the absence of antigen-presenting cells, far more so than the negative control irrelevant peptides in the T cell + Ag culture, likely suggesting degradation of LP into SP following immune cell death and release of proteases into the supernatant (**Figure 2C**).[50] In theory, proteolytic degradation of SP can diminish CD8 T cell stimulation, while proteolytic degradation of LP can either enhance or decrease stimulation, depending on the amino acid sequences of the resultant peptides (eg LP degradation into $E7_{(11-19)}$ SP might increase T cell stimulation). This phenomenon may explain the significant variation in IFNg production in the SP and LP groups across different experiments (**Figure 2C vs Figure 5A vs Figure 6**). In addition, it would reconcile significant IFNg variability across ECP permutations (**Figure 6**) despite the fact that SP-mediated T cell stimulation is independent of functional APC internalization and cross-presentation.[51] Cell passage through the ECP device itself may damage immune cells and cause the release of proteases. This theory also addresses LP's seemingly inconsistent generation of IFNg (**Figure 6**). LP requires functional internalization by APC and presentation to CD8 T cells and therefore should show a progressive increase in T cell stimulation as more DC-generating ECP components are incorporated into the experiment.[4,6,12,18,20] Instead, for example, the PLT-/TI- LP group produced significantly more IFNg than PLT+/TI+ LP and PLT-/TI+ LP groups (**Figure 6;** $p<0.0001$).

Overall, PBMC + T cell + Ag assay results suggested successful cross-presentation of the $E7_{(11-19)}$ tumor-relevant epitope to specifically activate CD8 T cells. Peptide stimulations (**Figures 5A, 6**) demonstrated varying degrees of stimulation with LP, as explained above. Tumor cell line stimulations were particularly successful with respect to SCC61 T+, confirming cross-presentation efficiency of tumor-derived E7 Ag (**Figures 5B-C, 6**). Tumor cell lines SCC61 T- (negative control) and SCC90 did not

produce significant quantities of IFNg. In fact, the SCC90 cell line that is reported to naturally express the E7 protein engendered a similar or inferior T cell stimulation as the SCC61 T- cell line without E7 expression (**Figure 6**). Because RT-PCR and immunoblotting was not completed at the time of this submission, E7 expression was not quantified across the tumor cell lines. SCC90's inferior antigenicity is likely a result of superior immune evasion strategies, including downregulation of MHCI, downregulation of E7 protein translation, and/or mutations of other components of cellular cross-presentation machinery.[2,27,31] In contrast, the SCC61 T+ line, theoretically expressing the highest amount of E7, was able to clearly able to demonstrate APC internalization and cross-presentation to epitope-specific T cells (**Figure 5B vs 5C**); this efficiency was maximized with the full TI effect (**Figure 6**). In other words, the presence of platelets, plate-passage, and overnight incubation significantly contributed to antigen cross-presentation (**Figure 5B vs 5C**; **Figure 6**), results in agreement with prior literature.[4,6,20]

Successful cross-presentation in peptide-based and tumor cell assays was supported by evidence of mature, inflammatory DC phenotype expression by monocytes following TI (**Figure 7**). In general, all immunogenic surface markers and intracellular chemokines were upregulated in TI-treated monocytes relative to fresh untreated monocytes. Moreover, the presence of platelets enhanced the expression of every inflammatory marker except MCP-1 (**Figure 7I**), further corroborating the importance of platelets in the TI/APC-maturation effect. Interestingly, monocytes of the tumor (SCC61 T+) overnight incubation group appeared to demonstrate the smallest increase in surface markers, and in fact, these cells displayed less MHCI (HLA-ABC) than fresh monocytes. However, this is not to suggest that monocytes co-incubated with SCC61 T+ cells did not mature into inflammatory DCs. Instead, these monocytes/MoDCs were likely in the process of phagocytosing large apoptotic tumor cells, and subsequently internalized large segments of their cell membranes displaying these markers.[52,53] Peptide pinocytosis or receptor-mediated endocytosis, which rely on internalizing a smaller proportion of the cell membrane, would likely have a significantly lesser effect on cell surface marker expression.[52,53] In contrast, internalization of whole tumors led to largest increase of inflammatory chemokine expressing monocytes/MoDCs

populations (CXCL5+ (>50%) and MCP-1+ (>33%)) confirming the immunogenicity of apoptotic whole tumors, perhaps through DAMP activation.[47]

Limitations and Future Directions

The initial results have been encouraging, demonstrating successful stimulation of antigen-specific T cells by apoptotic tumor cell-pulsed, ECP-treated antigen presenting cells. T cell stimulation experiments will be repeated to improve statistical power. Other HPV+ E7 expressing tumor cell lines, including cervical cancers[30], will be tested to further showcase ECP's ability to produce an antigen-specific immunogenic response across several malignancies. In the most clinically relevant in vitro model, we will attempt to reproduce our experimental setup using a fully autologous system of HNSCC patient PBMCs, surgically-removed tumors, and/or patient-derived tumor-infiltrating lymphocytes. If ECP is able to stimulate donor tumor-reactive T cells with patient-derived neoantigens, then such reactive cells should be double-positive for IFNg and PD-1, as previously shown for in vivo tumor targeting strategies.[3,36] Furthermore, these findings can be validated in murine in vivo tumor experiments, similar to past studies.[4,30]

Based on our current mechanistic understanding of ECP, we believe in its potential to treat the highly immunosuppressive HNSCC. Over 70 active HNSCC clinical trials involving checkpoint inhibitors directed against PD-1 and CTLA-4 are currently underway.[31] Though response rates to PD-1 inhibitors pembrolizumab and nivolumab remain below 20%, they have demonstrated dramatic improvements in median overall survival compared with standard of care therapy.[31] Nonetheless, absolute median survival is still low.[31] Thus, ECP offers a unique, exciting synergy with checkpoint inhibitors by directing an adaptive immune response across numerous undefined, patient-specific neoantigens[5] while simultaneously avoiding tumor-microenvironment mediated anergy.[2]

REFERENCES

1. Moskovitz JM, Moy J, Seiwert TY, Ferris RL. Immunotherapy for Head and Neck Squamous Cell Carcinoma: A Review of Current and Emerging Therapeutic Options. *Oncologist.* 2017;22(6):680-693.
2. Zolkind P, Dunn GP, Lin T, Griffith M, Griffith OL, Uppaluri R. Neoantigens in immunotherapy and personalized vaccines: Implications for head and neck squamous cell carcinoma. *Oral Oncol.* 2017;71:169-176.
3. Stevanovic S, Pasetto A, Helman SR, et al. Landscape of immunogenic tumor antigens in successful immunotherapy of virally induced epithelial cancer. *Science.* 2017;356(6334):200-205.
4. Ventura A, Vassall A, Robinson E, et al. Extracorporeal Photochemotherapy Drives Monocyte-to-Dendritic Cell Maturation to Induce Anticancer Immunity. *Cancer Res.* 2018;78(14):4045-4058.
5. Edelson RL. Mechanistic insights into extracorporeal photochemotherapy: efficient induction of monocyte-to-dendritic cell maturation. *Transfusion and apheresis science : official journal of the World Apheresis Association : official journal of the European Society for Haemapheresis.* 2014;50(3):322-329.
6. Girardi M, Schechner J, Glusac E, Berger C, Edelson R. Transimmunization and the evolution of extracorporeal photochemotherapy. *Transfusion and apheresis science : official journal of the World Apheresis Association : official journal of the European Society for Haemapheresis.* 2002;26(3):181-190.
7. Berger CL, Xu AL, Hanlon D, et al. Induction of human tumor-loaded dendritic cells. *Int J Cancer.* 2001;91(4):438-447.
8. Berger CL, Hanlon D, Kanada D, Girardi M, Edelson RL. Transimmunization, a novel approach for tumor immunotherapy. *Transfusion and apheresis science : official journal of the World Apheresis Association : official journal of the European Society for Haemapheresis.* 2002;26(3):205-216.
9. Ott PA, Hu Z, Keskin DB, et al. An immunogenic personal neoantigen vaccine for patients with melanoma. *Nature.* 2017;547(7662):217-221.
10. Draper LM, Kwong ML, Gros A, et al. Targeting of HPV16+ Epithelial Cancer Cells by TCR Gene Engineered T Cells Directed against E6. *Clin Cancer Res.* 2015;21(19):4431-4439.
11. Edelson R, Berger C, Gasparro F, et al. Treatment of cutaneous T-cell lymphoma by extracorporeal photochemotherapy. Preliminary results. *N Engl J Med.* 1987;316(6):297-303.
12. Berger C, Hoffmann K, Vasquez JG, et al. Rapid generation of maturationally synchronized human dendritic cells: contribution to the clinical efficacy of extracorporeal photochemotherapy. *Blood.* 2010;116(23):4838-4847.
13. Hart JW, Shiue LH, Shpall EJ, Alousi AM. Extracorporeal photopheresis in the treatment of graft-versus-host disease: evidence and opinion. *Ther Adv Hematol.* 2013;4(5):320-334.
14. Plumas J, Manches O, Chaperot L. Mechanisms of action of extracorporeal photochemotherapy in the control of GVHD: involvement of dendritic cells. *Leukemia.* 2003;17(11):2061-2062.

15. Steinman RM, Hawiger D, Nussenzweig MC. Tolerogenic dendritic cells. *Annu Rev Immunol.* 2003;21:685-711.
16. Kushwah R, Hu J. Dendritic cell apoptosis: regulation of tolerance versus immunity. *J Immunol.* 2010;185(2):795-802.
17. Edelson R, Wu Y, Schneiderman J. American council on ECP (ACE): Why now? *J Clin Apher.* 2018;33(4):464-468.
18. Durazzo TS, Tigelaar RE, Filler R, Hayday A, Girardi M, Edelson RL. Induction of monocyte-to-dendritic cell maturation by extracorporeal photochemotherapy: initiation via direct platelet signaling. *Transfusion and apheresis science : official journal of the World Apheresis Association : official journal of the European Society for Haemapheresis.* 2014;50(3):370-378.
19. Tambur AR, Ortegel JW, Morales A, Klingemann H, Gebel HM, Tharp MD. Extracorporeal photopheresis induces lymphocyte but not monocyte apoptosis. *Transplant Proc.* 2000;32(4):747-748.
20. Kibbi N, Sobolev O, Girardi M, Edelson RL. Induction of anti-tumor CD8 T cell responses by experimental ECP-induced human dendritic antigen presenting cells. *Transfusion and apheresis science : official journal of the World Apheresis Association : official journal of the European Society for Haemapheresis.* 2016;55(1):146-152.
21. Hanlon DJ, Berger CL, Edelson RL. Photoactivated 8-methoxypsoralen treatment causes a peptide-dependent increase in antigen display by transformed lymphocytes. *Int J Cancer.* 1998;78(1):70-75.
22. Futterleib JS, Feng H, Tigelaar RE, Choi J, Edelson RL. Activation of GILZ gene by photoactivated 8-methoxypsoralen: potential role of immunoregulatory dendritic cells in extracorporeal photochemotherapy. *Transfusion and apheresis science : official journal of the World Apheresis Association : official journal of the European Society for Haemapheresis.* 2014;50(3):379-387.
23. Rao V, Saunes M, Jorstad S, Moen T. In vitro experiments demonstrate that monocytes and dendritic cells are rendered apoptotic by extracorporeal photochemotherapy, but exhibit unaffected surviving and maturing capacity after 30 Gy gamma irradiation. *Scand J Immunol.* 2008;68(6):645-651.
24. Holtick U, Marshall SR, Wang XN, Hilkens CM, Dickinson AM. Impact of psoralen/UVA-treatment on survival, activation, and immunostimulatory capacity of monocyte-derived dendritic cells. *Transplantation.* 2008;85(5):757-766.
25. Tran Janco JM, Lamichhane P, Karyampudi L, Knutson KL. Tumor-infiltrating dendritic cells in cancer pathogenesis. *J Immunol.* 2015;194(7):2985-2991.
26. Girardi M, Berger CL, Wilson LD, et al. Transimmunization for cutaneous T cell lymphoma: a Phase I study. *Leuk Lymphoma.* 2006;47(8):1495-1503.
27. Moreira J, Tobias A, O'Brien MP, Agulnik M. Targeted Therapy in Head and Neck Cancer: An Update on Current Clinical Developments in Epidermal Growth Factor Receptor-Targeted Therapy and Immunotherapies. *Drugs.* 2017;77(8):843-857.
28. Vermorken JB, Mesia R, Rivera F, et al. Platinum-based chemotherapy plus cetuximab in head and neck cancer. *N Engl J Med.* 2008;359(11):1116-1127.
29. Global Burden of Disease Cancer C, Fitzmaurice C, Allen C, et al. Global, Regional, and National Cancer Incidence, Mortality, Years of Life Lost, Years Lived With Disability, and Disability-Adjusted Life-years for 32 Cancer Groups, 1990 to 2015: A Systematic Analysis for the Global Burden of Disease Study. *JAMA Oncol.* 2017;3(4):524-548.

30. Jin BY, Campbell TE, Draper LM, et al. Engineered T cells targeting E7 mediate regression of human papillomavirus cancers in a murine model. *JCI Insight.* 2018;3(8).
31. Santuray RT, Johnson DE, Grandis JR. New Therapies in Head and Neck Cancer. *Trends Cancer.* 2018;4(5):385-396.
32. Kreimer AR, Clifford GM, Boyle P, Franceschi S. Human papillomavirus types in head and neck squamous cell carcinomas worldwide: a systematic review. *Cancer Epidemiol Biomarkers Prev.* 2005;14(2):467-475.
33. Garcia-Bates TM, Kim E, Concha-Benavente F, et al. Enhanced Cytotoxic CD8 T Cell Priming Using Dendritic Cell-Expressing Human Papillomavirus-16 E6/E7-p16INK4 Fusion Protein with Sequenced Anti-Programmed Death-1. *J Immunol.* 2016;196(6):2870-2878.
34. Hinrichs CS, Rosenberg SA. Exploiting the curative potential of adoptive T-cell therapy for cancer. *Immunol Rev.* 2014;257(1):56-71.
35. Lee SJ, Yang A, Wu TC, Hung CF. Immunotherapy for human papillomavirus-associated disease and cervical cancer: review of clinical and translational research. *J Gynecol Oncol.* 2016;27(5):e51.
36. Yossef R, Tran E, Deniger DC, et al. Enhanced detection of neoantigen-reactive T cells targeting unique and shared oncogenes for personalized cancer immunotherapy. *JCI Insight.* 2018;3(19).
37. Gonzalez-Galarza FF, Christmas S, Middleton D, Jones AR. Allele frequency net: a database and online repository for immune gene frequencies in worldwide populations. *Nucleic Acids Res.* 2011;39(Database issue):D913-919.
38. Riemer AB, Keskin DB, Zhang G, et al. A conserved E7-derived cytotoxic T lymphocyte epitope expressed on human papillomavirus 16-transformed HLA-A2+ epithelial cancers. *J Biol Chem.* 2010;285(38):29608-29622.
39. Khallouf H, Grabowska AK, Riemer AB. Therapeutic Vaccine Strategies against Human Papillomavirus. *Vaccines (Basel).* 2014;2(2):422-462.
40. Saluja SS, Hanlon DJ, Sharp FA, et al. Targeting human dendritic cells via DEC-205 using PLGA nanoparticles leads to enhanced cross-presentation of a melanoma-associated antigen. *Int J Nanomedicine.* 2014;9:5231-5246.
41. Gubanova E, Brown B, Ivanov SV, et al. Downregulation of SMG-1 in HPV-positive head and neck squamous cell carcinoma due to promoter hypermethylation correlates with improved survival. *Clin Cancer Res.* 2012;18(5):1257-1267.
42. Ranieri E, Popescu I, Gigante M. CTL ELISPOT assay. *Methods Mol Biol.* 2014;1186:75-86.
43. Woodhead VE, Stonehouse TJ, Binks MH, et al. Novel molecular mechanisms of dendritic cell-induced T cell activation. *Int Immunol.* 2000;12(7):1051-1061.
44. Gros A, Parkhurst MR, Tran E, et al. Prospective identification of neoantigen-specific lymphocytes in the peripheral blood of melanoma patients. *Nat Med.* 2016;22(4):433-438.
45. Pasetto A, Gros A, Robbins PF, et al. Tumor- and Neoantigen-Reactive T-cell Receptors Can Be Identified Based on Their Frequency in Fresh Tumor. *Cancer Immunol Res.* 2016;4(9):734-743.
46. Duraiswamy J, Ibegbu CC, Masopust D, et al. Phenotype, function, and gene expression profiles of programmed death-1(hi) CD8 T cells in healthy human adults. *J Immunol.* 2011;186(7):4200-4212.

47. Hernandez C, Huebener P, Schwabe RF. Damage-associated molecular patterns in cancer: a double-edged sword. *Oncogene.* 2016;35(46):5931-5941.
48. Ramos CA, Narala N, Vyas GM, et al. Human papillomavirus type 16 E6/E7-specific cytotoxic T lymphocytes for adoptive immunotherapy of HPV-associated malignancies. *J Immunother.* 2013;36(1):66-76.
49. Perkey E, Maillard I. New Insights into Graft-Versus-Host Disease and Graft Rejection. *Annu Rev Pathol.* 2018;13:219-245.
50. Ryan BJ, Henehan GT. Avoiding Proteolysis During Protein Purification. *Methods Mol Biol.* 2017;1485:53-69.
51. Schott E, Bertho N, Ge Q, Maurice MM, Ploegh HL. Class I negative CD8 T cells reveal the confounding role of peptide-transfer onto CD8 T cells stimulated with soluble H2-K-b molecules. *P Natl Acad Sci USA.* 2002;99(21):13735-13740.
52. Buys SS, Kaplan J. Effect of phagocytosis on receptor distribution and endocytic activity in macrophages. *J Cell Physiol.* 1987;131(3):442-449.
53. Gul N, van Egmond M. Antibody-Dependent Phagocytosis of Tumor Cells by Macrophages: A Potent Effector Mechanism of Monoclonal Antibody Therapy of Cancer. *Cancer Res.* 2015;75(23):5008-5013.

FIGURES

Figure 1. Flow cytometry confirms large viable populations of anti-HPV16 E7$_{(11-20)}$ and anti-HPV16 E7$_{(11-20)}$ CD8 T cells following rapid expansion (REP). Common abbreviations/stains: SSC = side scatter; FSC = forward scatter; zombie-APC-Cy7 (live-dead); CD8-PacBlue; CD3-APC. **(A)** REP generated a viable 67% pure anti-HPV16 E7$_{(11-20)}$ CD8 T cell population. Specific stain: E7$_{(11-20)}$ dextramer-PE. **(B)**. REP generated a viable ~95% pure anti-HPV16 E7$_{(11-19)}$ CD8 T cell population. Specific stains: murineTCR-beta (mTCR-beta) –FITC; CD4-PE-Cy5.5.

A.

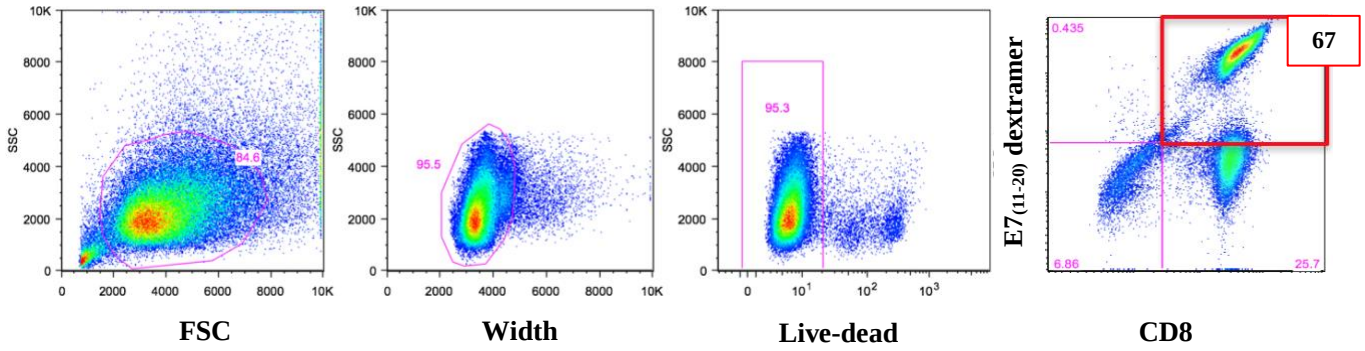

B.

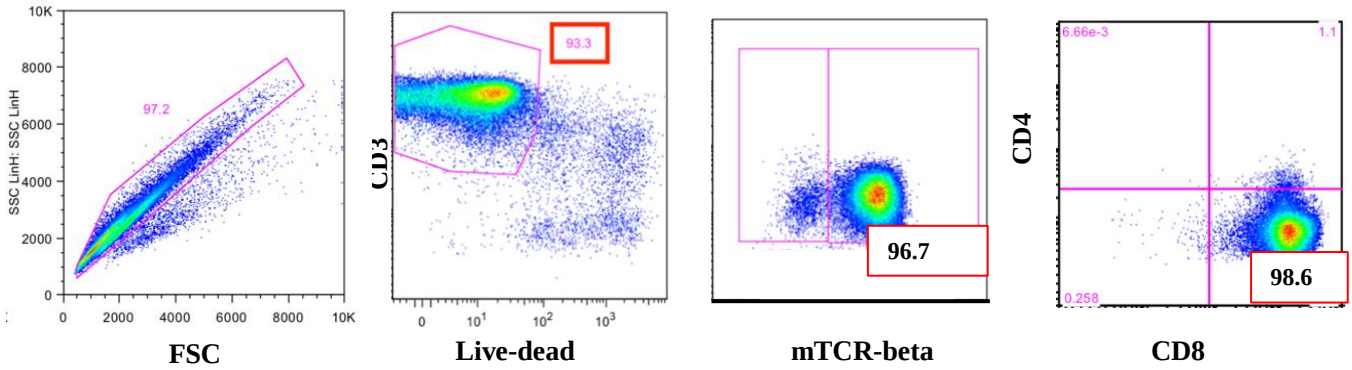

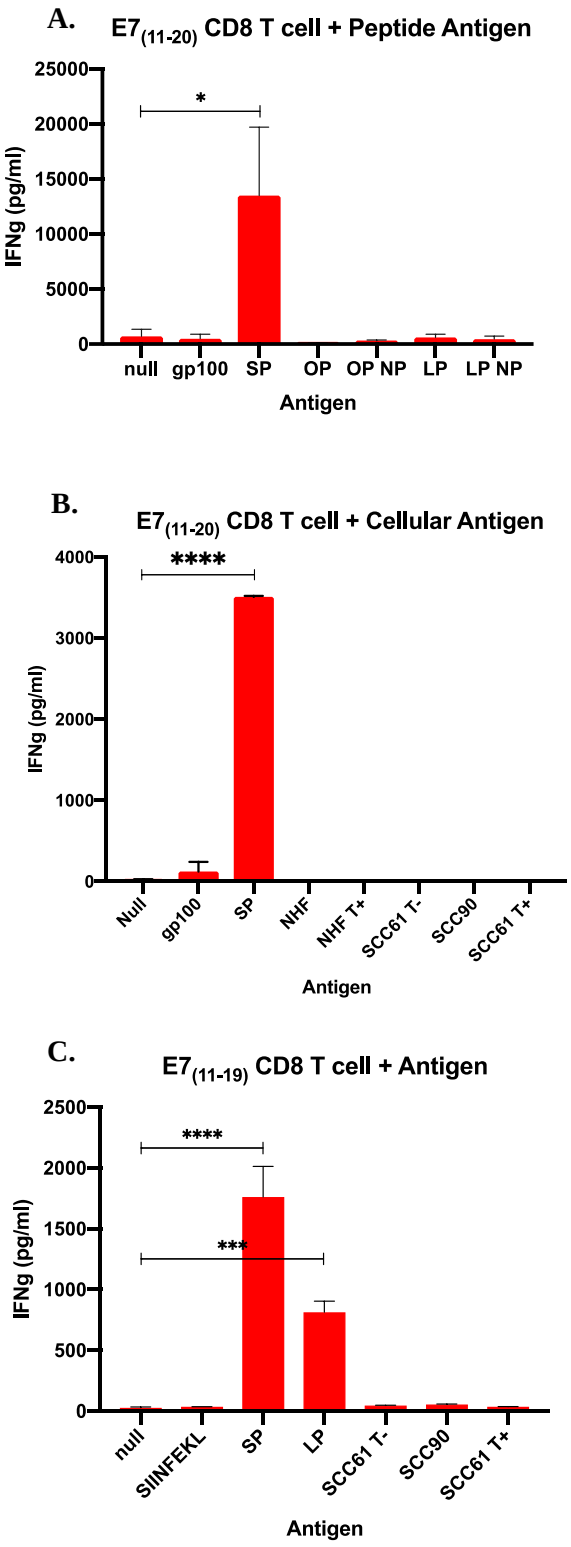

Figure 2. IFNg ELISA results following 72 hour CD8 T cell incubation with various antigens. No antigen presenting cell is present and thus, only short peptide (SP) should directly be able to stimulate the TCR. Cognate SP appropriately stimulates CD8 T cells. Statistically significant IFNg production is relative to the T cell only group without antigen (ie "null"). Statistically significant (ie *$p<0.05$) bars are displayed. (**A**) $E7_{(11-20)}$ CD8 T cells are exclusively stimulated in the presence of $E7_{(11-20)}$ SP and not other peptides/nanoparticle combinations, $p=0.012$. (**B**) $E7_{(11-20)}$ CD8 T cells are exclusively stimulated in the presence of corresponding short peptide (SP) again, ($p<0.0001$), and not cell lines. (**C**) $E7_{(11-19)}$ CD8 T cells are stimulated in the presence of $E7_{(11-19)}$ SP (****$p<0.0001$) and LP (***$p<0.001$), but not other peptides and cell lines. LP likely directly stimulated TCRs following proteolytic degradation into SP (see discussion).

A.

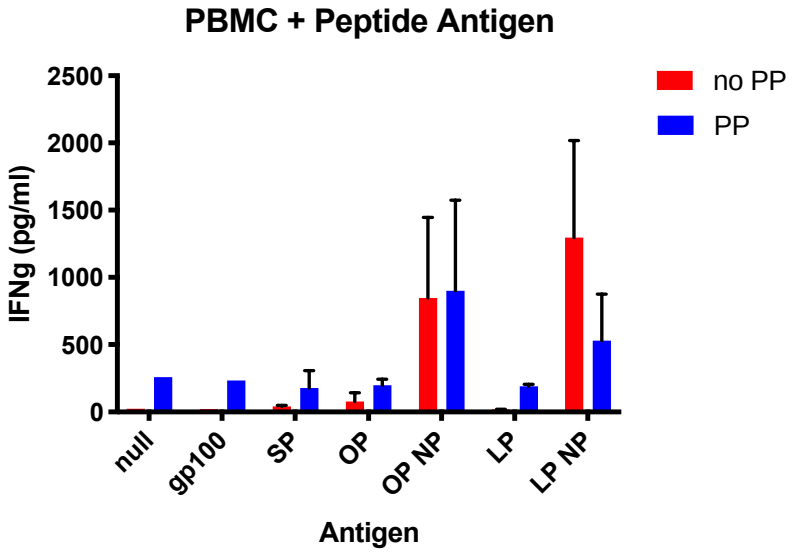

B.

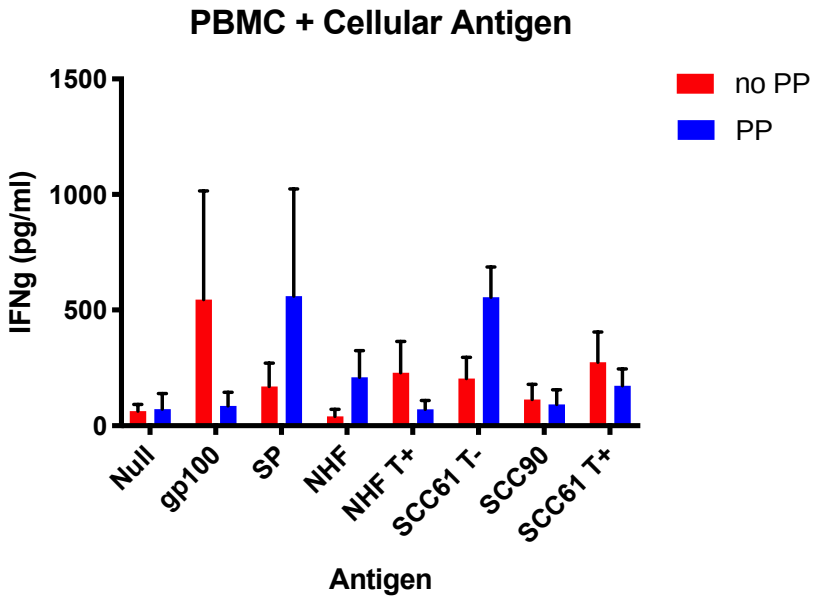

Figure 3. IFNg ELISA results following 72 hour PBMC incubation with various antigens (Ags) during testing of the E7$_{(11\text{-}20)}$ system. Because there is no epitope-specific CD8 T cell line to respond to Ag cross-presentation, PBMC + Ag IFNg provides a sense of non-epitope related IFNg production. Results above are from 3 different donors. Plate-passaged PBMCs (PP) are compared with non-plate-passaged PBMCS (no PP). PLGA nanoparticle (NP) encapsulated peptides are included. (**A**) In the PBMC + peptide Ag incubation, maximal IFNg was 1272pg/ml from the LP NP group. (**B**) In the PBMC + cellular Ag incubation, maximal IFNg was 560pg/ml from the SP group. These values served as "background noise" (dotted lines) for Figure 4.

A.

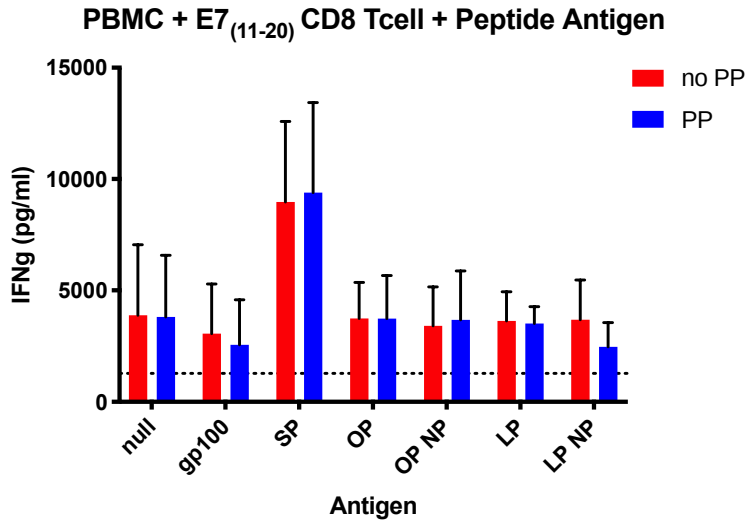

B.

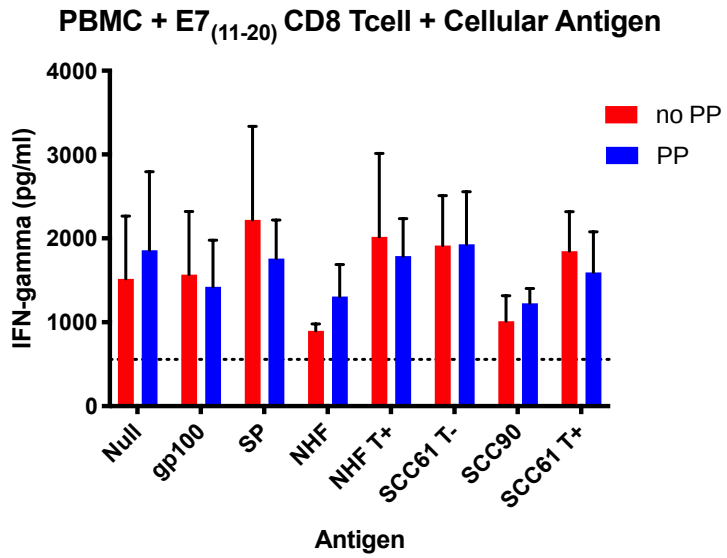

Figure 4. IFNg ELISA results following 72 hour co-culture of PBMC and CD8 T cell with various antigens (Ags) during testing of the E7$_{(11-20)}$ system. Overall, there was nonspecific IFNg production in the E7$_{(11-20)}$ system. IFNg should be released upon APC internalization/processing/cross-presentation of E7+ antigen (Ag) or direct stimulation of CD8 T cell receptor (ie with short peptide). Antigens: gp100 (melanoma peptide; a negative control); E7$_{(11-20)}$ short peptide (SP); E7$_{(1-30)}$ long peptide (LP); normal human fibroblast and fibroblasts expressing E6 and E7 proteins (NHF, NHF T+ respectively); SCC90 (naturally expressing E7); SCC61 T- and SCC61 T+ (naturally non-E7 expressing and transfected to express high levels of E7, respectively). PLGA nanoparticle (NP) encapsulated peptides are included. Statistically significant IFNg production is relative to the group without antigen (ie "null"). (**A**) There was non-specific IFNg production in E7+ peptide Ag sources ($p>0.98$). The nanoparticle effect did not enhance Ag cross-presentation ($p>0.98$). The plate-passage effect did not enhance T cell stimulation ($p>0.98$). (**B**) There was non-specific IFNg production in cellular E7+ Ag sources ($p>0.98$). The plate-passage effect did not enhance T cell stimulation ($p>0.98$).

A.

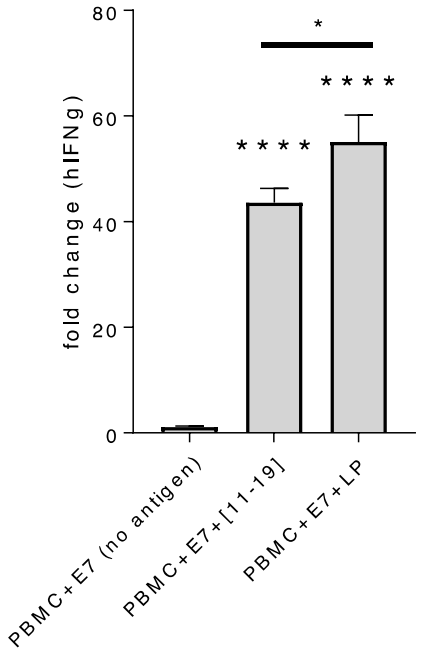

Figure 5. Preliminary IFNg ELISA results of the $E7_{(11-19)}$ system following overnight PBMC-antigen incubation and 72 hour PBMC + CD8 T cell co-culture. (A) PBMC + $E7_{(11-19)}$ CD8 T cell ("PBMC + E7") was incubated with $E7_{(11-19)}$ short peptide ("[11-19]") or $E7_{(1-30)}$ long peptide ("LP"). Relative to the no antigen control group, addition of SP and LP resulted in significant T cell stimulation (>40x and >50x IFNg, respectively; ****p<0.0001 for both). LP produced significantly more IFNg than SP (*p<0.05). **(B)** PBMC + $E7_{(11-19)}$ CD8 T cell + E7 expressing SCC61 (SCC61 T+) or control non-E7 expressing SCC61(SCC61 T-) **(C)** are compared. The effects of platelet depletion ("pl^-") and monocyte isolation ("$mono^+$") were also investigated. An antigen-specific CD8 T cell response was confirmed by significant IFNg production in only the SCC61T+ groups; specifically, only platelet-containing ("pl+") PBMC and monocyte SCC61 T+ groups significantly produced IFNg (p<0.0001). These results underscore critical ECP variables (ie monocytes as the antigen presenting cell progenitor and platelets) needed for efficient antigen cross-presentation. Non-statistically significant differences ("n.s."; p>0.05) are highlighted with bars.

2

B.

C.

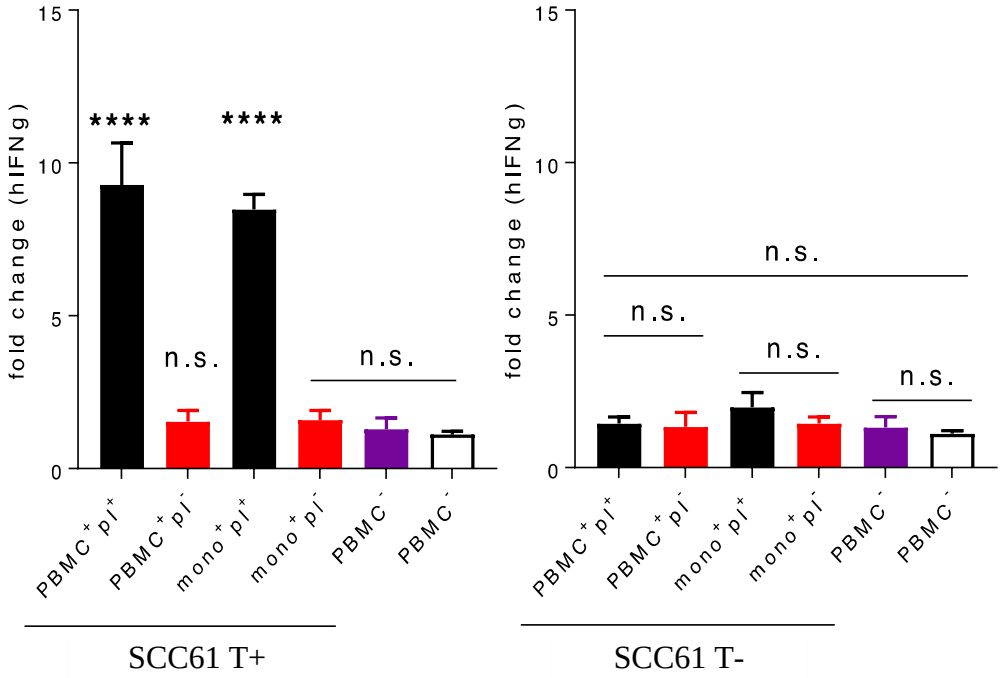

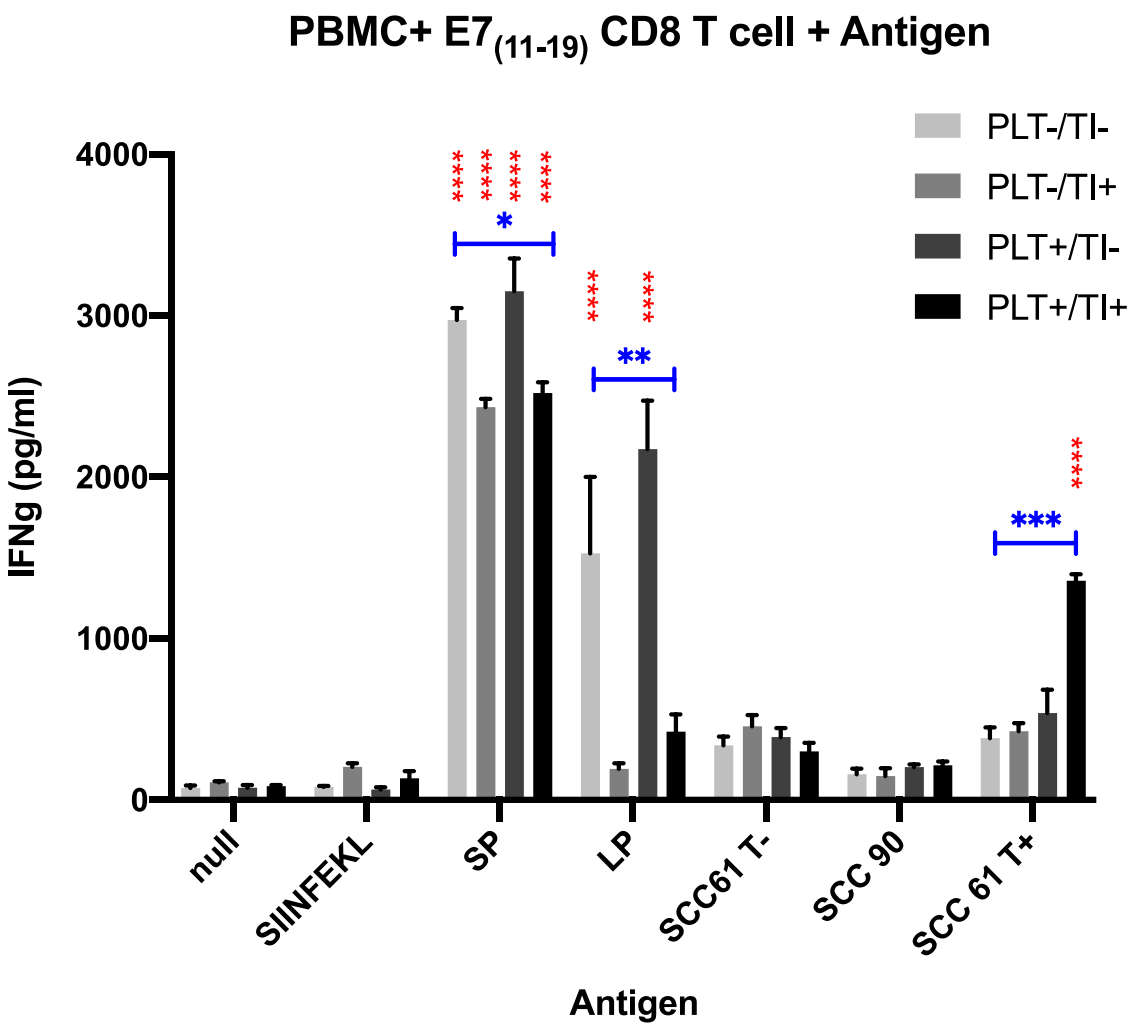

Figure 6. IFNg ELISA results following 72 hour PBMC incubation with various antigens (Ags) during testing of the E7$_{(11\text{-}19)}$ system. Overall, co-cultures suggested Ag-specific CD8 T cell stimulation. Critical Transimmunization (TI) components were investigated including platelet depletion ("PLT-") and the absence of TI (ie no plate-passage of PBMCs & no Ag overnight incubation). Antigens: SIINFEKL (negative peptide control); E7$_{(11\text{-}19)}$ short peptide (SP); E7$_{(1\text{-}30)}$ long peptide (LP); SCC90 (naturally expressing E7); SCC61 T- and SCC61 T+ (naturally non-E7 expressing and transfected to express high levels of E7, respectively). Negative control groups (null and SIINFEKL) produce comparably low IFNg ($p>0.78$). Statistically significant IFNg production with respect to the corresponding negative control group is denoted in red asterisks above the experimental group. Peptide groups were compared to the null group while tumor groups were compared to SCC61 T- (E7 negative) to account for potential DAMP (Damage-associated Molecular Patterns) non-Ag specific stimulation from dying tumor cells. Blue asterisks denote statistically significant differences *within* an Ag group, to determine whether TI variables affect Ag cross-presentation. With respect to peptides, SP (positive control) and LP (PLT-/TI- & PLT+/TI-) groups produced significant IFNg ($p<0.0001$). With respect to tumor cells, only the PLT+/TI+ SCC61 T+ group produced high levels of IFNg ($p<0.0001$), while SCC90 produced comparable ($p>0.09$) or less (PLT-/TI+, $p=0.039$) IFNg than corresponding SCC61 T- groups. TI protocol modifications resulted in significant differences *within* SP ($p<0.017$) and LP ($p<0.003$) groups, but not according to the expected trend (see discussion). TI protocol modifications results in significant differences *within* the SCC61 T+ group; following the expected trend, PLT+/TI+ resulted in superior cross presentation relative to PLT+/TI- ($p=0.001$), PLT-/TI+ ($p<0.0001$), and PLT-/TI- ($p<0.0001$). *$p<0.05$; **$p<0.01$; ***$p<0.001$; ****$p<0.0001$.

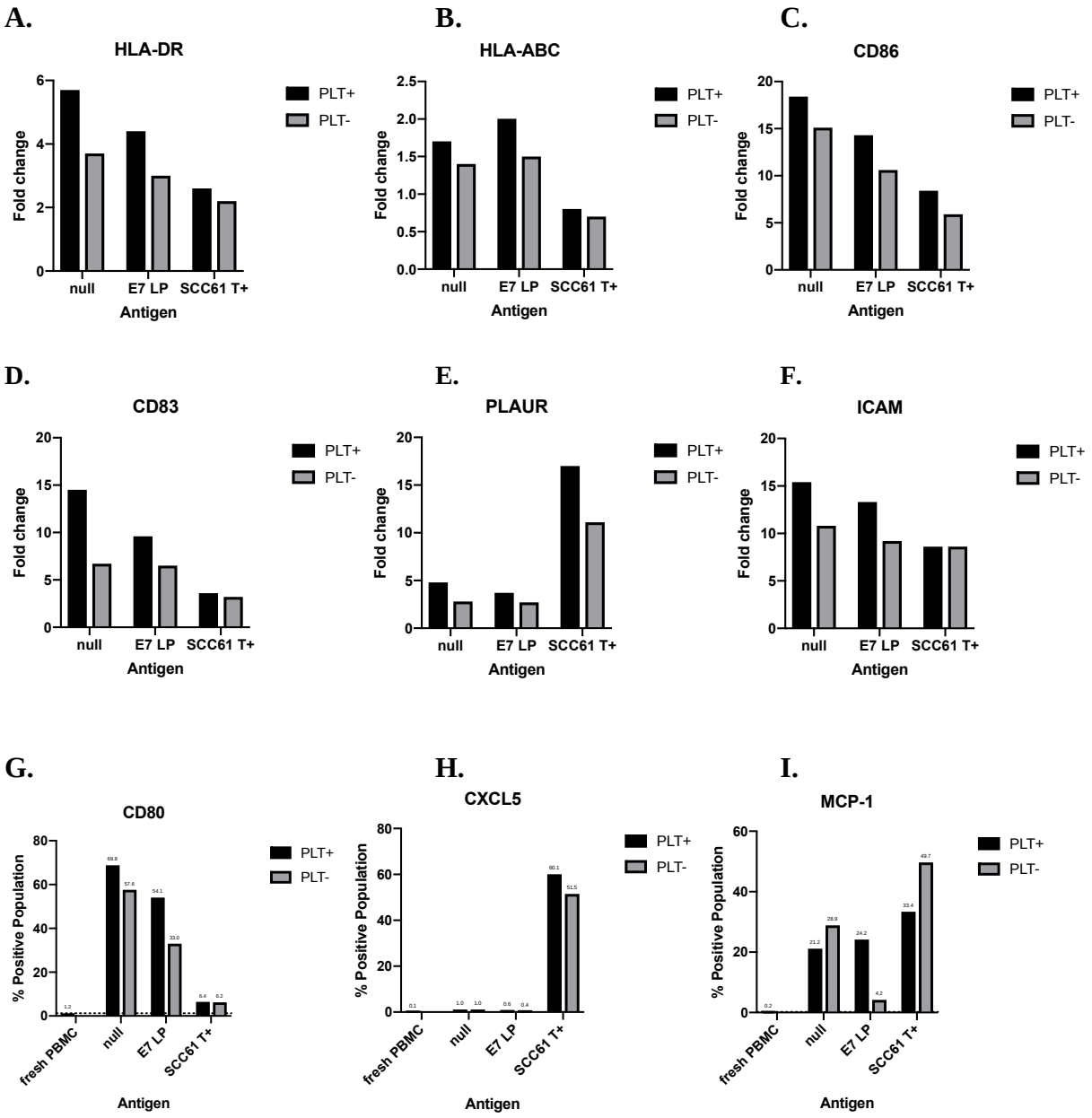

Figure 7. **Inflammatory maturation MoDC markers were quantified using flow cytometry.** After overnight incubation, inflammatory markers of platelet-depleted (PLT-) and platelet-containing (PLT+) monocytes that had undergone TI (ie plate-passage and overnight incubation) with long peptide (LP) or with SCC61 T+ were compared to monocytes from fresh PBMCs. Monocytes were identified on the basis of CD14+/CD11c+ populations from live, singlet PBMCs. Surface markers (HLA-DR, HLA-ABC, CD-86, CD-83, PLAUR, ICAM) were plotted as fold-change in mean fluorescent intensity (MFI) relative to fresh monocytes (ie value of 1 suggests MFI equal to that of fresh monocytes). Percentage of positive monocytes was used to track populations expressing intracellular chemokines or surface CD80. Overall, platelet and TI factors generally resulted in an increased expression of every inflammatory marker (exceptions: MCP-1 for platelets, HLA-ABC for TI). Notably, SCC61 T+ monocytes showed distinct upregulations in CXCL5 and PLAUR but a relative decreased expression in surface markers (see discussion).

Figure 8. T cells upregulate PD-1 following OKT-3/IL-2 stimulation. These results suggest a working system to track patients' unknown neoantigen-reactive T cells in future experiments, as previously described in the literature. PD-1 expression in T cells following 2 day stimulation of PBMCs with OKT-3 (30ul of 1mg/ml stock) and 1300IU/ml IL-2 ("Stim(+)") was compared to 2 day unstimulated PBMCs ("Stim(-)"). FMO = fluorescence minus one. Ab = full staining panel. PD-1 positivity was calculated as the difference between Ab and FMO per population. For CD8 T cells, stimulation resulted in a 43% increase in the PD-1+ population (7% PD-1+ in unstimulated cells versus 50% in stimulated cells). For CD4 T cells, stimulation resulted in a 45% increase in the PD-1+ population (12% PD-1+ in unstimulated cells versus 57% in stimulated cells). Stains: PD-1-PacBlue, live-dead "zombie"-APC-Cy7, CD3-PE, CD4-APC, CD8-FITC. FSC = forward scatter; SSC = side scatter.

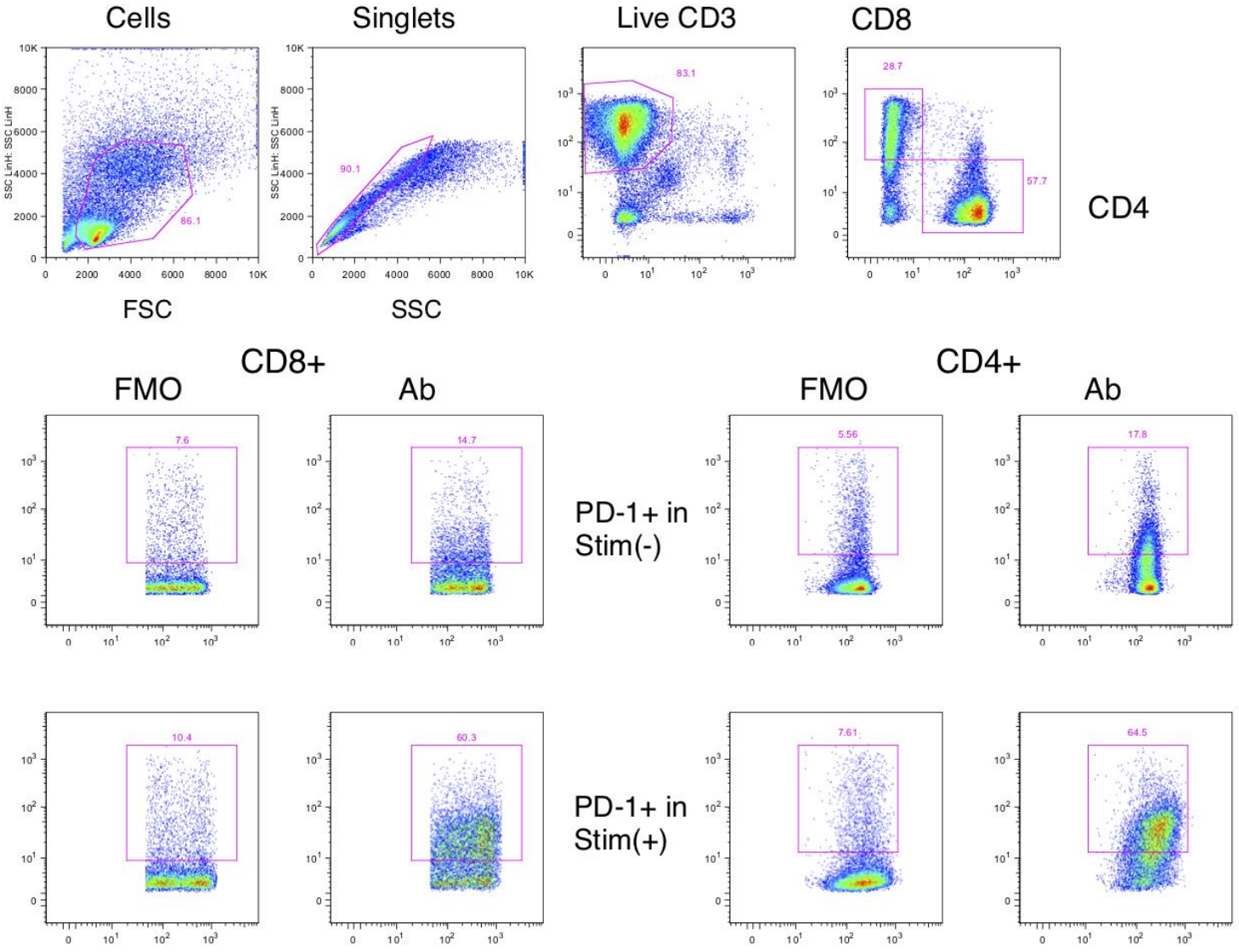

Supplementary Figure 1. **Schematic for CD8 T cell transduction, purification, and rapid expansion.** CD8 T cells were isolated from a healthy HLA-A2+ donor and transduced with an MSGV1 retrovirus encoding the $E7_{(11-19)}$ T cell receptor (TCR) plasmid. After incubation with the virus, CD8 T cells should co-express high avidity $E7_{(11-19)}$ TCR and can be identified based on the murine TCR-β (mTCRb) constant region. The transduced population of CD8 T cells was sorted with flow cytometry for CD3/CD8/mTCRb triple positivity and subsequently rapidly expanded. Thus, a large, high purity $E7_{(11-19)}$ CD8 T cell population was produced.

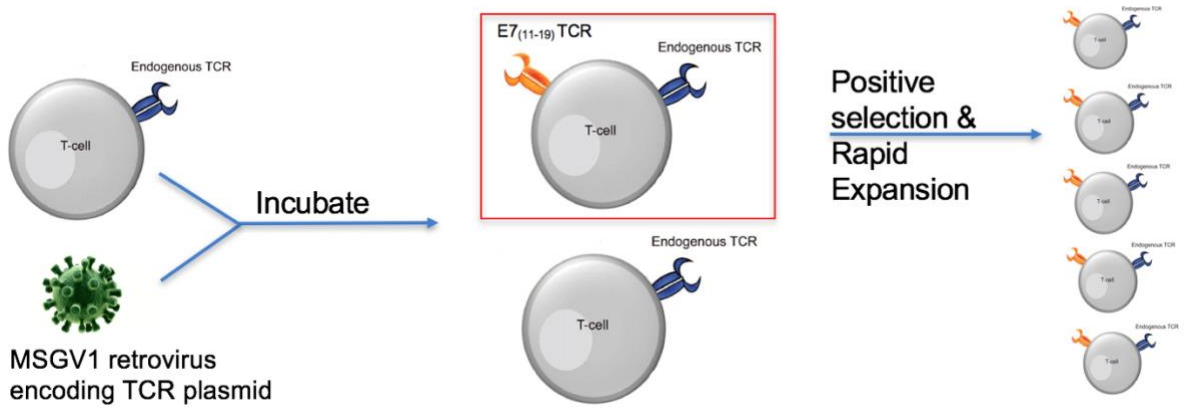

Supplementary Figure 2. Schematic for Transimmunization (TI) Experiments. PBMCs, containing antigen-presenting cell (APC) progenitors, and platelets (PLTs) are isolated from an HLA-A2+ donor. In tumor cell antigen groups, PUVA-treated tumor cells are plate-passaged with PBMCs. In peptide antigen groups, peptides are added to the overnight incubation dish containing PBMCs after plate passage. For both tumor cell and peptide antigen groups, after overnight incubation, PBMCs are co-cultured with epitope-specific CD8 T cells for 72 hours in 96-well plates. After this period, supernatant is collected for IFNg ELISA. If APC cross-presentation is successful, then stimulated CD8 T cells should produce IFNg.